retardation, genitourinary defects including cryptorchidism in males, and bleeding diathesis due to factor XI deficiency. The incidence of this syndrome is estimated to be 1 in 1,000–2,500 live births. LEOPARD (multiple *l*entigines, *e*lectrocardiographic conduction abnormalities, *o*cular hypertelorism, *p*ulmonary stenosis, *a*bnormal genitalia, *r*etardation of growth, and sensorineural *d*eafness) syndrome (MIM# 151100) is known to be a NS-related disorder [Digilio et al., 2002]. The features of NS overlap with those of Costello syndrome and cardio-facio-cutaneous (CFC) syndrome. Patients with Costello syndrome (MIM# 218040) show distinctive facial features, mental retardation, high birth weight, neonatal feeding problems, curly hair, nasal papillomata, deep skin creases at palms and soles, and hypertrophic cardiomyopathy [Hennekam, 2003]. CFC syndrome (MIM# 115150) is characterized by distinctive facial features, mental retardation, heart defects (PS, atrial septal defect [ASD], and hypertrophic cardiomyopathy), and ectodermal abnormalities such as sparse, friable hair, hyperkeratotic skin lesions, and a generalized ichthyosis-like condition [Reynolds et al., 1986].

The molecular pathogenesis of these syndromes has been investigated. Tartaglia et al. [2001] have identified missense mutations in *PTPN11*, a gene encoding protein tyrosine phosphatase (PTP) SHP-2, in 45% of clinically diagnosed NS patients. Specific mutations in *PTPN11* has been identified in patients with LEOPARD syndrome [Digilio et al., 2002]. In 2005, we identified *HRAS* germline mutations in patients with Costello syndrome [Aoki et al., 2005]. Mutations in *KRAS*, *BRAF*, and *MAP2K1/2* have been identified in those with CFC syndrome [Niihori et al., 2006; Rodriguez-Viciana et al., 2006]. Mutations in *KRAS* and *SOS1* have also been identified in patients with NS [Roberts et al., 2007; Schubbert et al., 2006; Tartaglia et al., 2007]. Mutations in *NF1* and *SPRED1* have been identified in patients with neurofibromatosis type I (MIM# 162200) [Brems et al., 2007]. These findings suggest that dysregulation of the RAS/RAF/MEK/ERK pathway causes NS and related disorders, and thus it has been suggested that these syndromes be comprehensively termed the RAS/MAPK syndromes [Aoki et al., 2008] or the neuro-cardio-facial-cutaneous syndrome [Bentires-Alj et al., 2006].

In 2007, gain-of-function mutations in *RAF1* were identified in 3–17% of patients with NS and two patients with LEOPARD syndrome [Pandit et al., 2007; Razzaque et al., 2007]. RAF1 is a member of the RAF serine–threonine kinase family and transmits the upstream RAS signaling to downstream MEK and ERK. RAF1, ARAF, and BRAF share three conserved regions, CR1, CR2, and CR3 [Mercer and Pritchard, 2003]. Mutations in *BRAF* identified in patients with CFC syndrome are clustered in CR1 and CR3 domains [Aoki et al., 2008]. In contrast, reported *RAF1* mutations in NS and LEOPARD syndrome were located in the CR2 domain and some mutations were located in CR3 domain. These mutants had enhanced RAF1 kinase activities and most mutations, but not all, showed enhanced phosphorylation of ERK1/2 [Pandit et al., 2007; Razzaque et al., 2007]. Pandit et al. [2007] suggested that RAF1 mutations might interfere with RAF1 phosphorylation at serine 259 as well as with 14-3-3 interaction, and reported that p.P261S did not bind to 14-3-3. However, the mechanisms of RAF1 activation in mutants remain unexplained.

In the present study, we analyzed the *RAF1* gene in 119 patients with NS and related phenotypes without mutations in *PTPN11*, *HRAS*, *KRAS*, *BRAF*, *MAP2K1/2*, and *SOS1*. Detailed clinical manifestations in our new patients with *RAF1* mutations were evaluated, and those in patients with *RAF1 KRAS*, *PTPN11*, and *SOS1* mutations previously reported by us and others were examined. Furthermore, we explored the molecular mechanisms by which RAF1 mutants are activated.

Materials and Methods

Patients

One hundred nineteen patients with NS or related phenotypes were recruited. The primary diagnoses made by clinical dysmorphologists and general pediatricians were as follows: 44 patients with NS, 46 patients with CFC syndrome, 25 patients with Costello syndrome, and 4 patients with atypical phenotypes. No mutations in *PTPN11*, *HRAS*, *KRAS*, *BRAF*, *MAP2K1*, *MAP2K2*, or *SOS1* were identified in these patients. Control DNA was obtained from 105 healthy Japanese individuals. Control DNA from 105 healthy Caucasian individuals was purchased from Coriell Cell Repositories (Camden, NJ). This study was approved by the Ethics Committee of Tohoku University School of Medicine. We obtained informed consent from all subjects involved in the study and specific consent for photographs from six patients.

Mutation Analysis in *RAF1*

Genomic DNA was isolated from the peripheral blood leukocytes of the patients. Each exon with flanking intronic sequences in *RAF1* was amplified with primers based on GenBank sequences (Supp. Table S1; GenBank accession no. NC_000003.10). The M13 reverse or forward sequence was added to the 5′ end of the polymerase chain reaction (PCR) primers for use as a sequencing primer. PCR was performed in 30 μl of a solution containing 10 mM Tris-HCl (pH 8.3), 50 mM KCl, 1.5 mM $MgCl_2$, 0.2 mM dNTP, 10% (v/v) DMSO, 24 pmol of each primer, 100 ng genomic DNA, and 1.5 units of Taq DNA polymerase. The reaction conditions consisted of 35 cycles of denaturation at 94°C for 15 sec, annealing at 55°C for 15 sec, and extension at 72°C for 40 sec. The products were gel-purified and sequenced on an ABI PRISM 310 or 3130 automated DNA sequencer (Applied Biosystems, Foster City, CA).

Determination of the RAF1 Phosphorylation Status

The expression construct, including a *RAF1* cDNA (pUSEamp-*RAF1*), was purchased from Millipore (Billerica, MA). A Myc-tag was introduced at the 5′ terminus of the cDNA by PCR and the PCR product was subcloned into pCR4-TOPO (Invitrogen, Carlsbad, CA). The entire cDNA was verified by sequencing. A single-base substitution resulting in p.H103Q, p.R191I, p.S257L, p.S259F, p.P261A, p.N262K, or p.S427G was introduced using a QuickChange Site-Directed Mutagenesis Kit (Stratagene, La Jolla, CA). All mutant constructs were verified by sequencing. The Myc-tagged wild-type *RAF1* cDNA and mutant cDNAs were digested with *Eco*RI and *Eco*RV and subcloned into the *Eco*RI–*Eco*RV site of the pUSEamp-*RAF1*.

COS7 cells were purchased from the American Type Culture Collection (ATCC, Rockville, MD). Cells were maintained in DMEM containing 10% fetal calf serum (FCS), 50 U/ml penicillin, and 50 μg/ml streptomycin. COS7 cells were seeded at 1×10^5 cells per 6-cm dish, and 24 hr later, 2.0 μg of pUSE vectors encoding one of the wild-type (WT) or mutant RAF1 cDNAs were transfected using 8 μl of PLUS Reagent and 12 μl of Lipofectamine Reagent (Invitrogen). After 3 hr, the medium was replaced to complete medium. After 48-hr culture, cells were scraped and collected by centrifugation after two washes with phosphate-buffered saline

(PBS). Lysates were prepared in 100-μl lysis buffer (10 mM Tris-HCl pH 8.0 and 1% SDS) and boiled for 3 min. The DNA was sheared with a syringe. The lysates were centrifuged at 14,000 × *g* for 15 min at 4°C and protein concentration was determined by Bradford assay. Thirty micrograms of protein was subjected to SDS-polyacrylamide gel electrophoresis (5–20% gradient gel) (ATTO, Tokyo, Japan), transferred to nitrocellulose membrane, and probed with anti-Myc antibody and phospho-specific RAF1 antibodies (Cell Signaling, Danvers, MA). All the membranes were visualized using a Western Lightning ECL-Plus Kit (Perkin-Elmer, Norwalk, CT). The following antibodies were used for Western blotting: anti-Myc (9E10, Santa Cruz Biotech, Santa Cruz, CA), antiphospho-c-Raf (S259) (Cell Signaling), antiphospho-c-Raf (S338) (Millipore), antiphospho-c-Raf (S289/296/301) (Cell Signaling), antiphospho-c-Raf (S621) (Millipore), and antineomycin phosphotransferase II (Millipore).

For immunoprecipitation, lysates were prepared in 1 ml of ice-cold RIPA buffer (50 mM Tris-HCl pH 7.5, 150 mM NaCl, 1 mM EDTA, 1:100 protease inhibitor (Sigma, St. Louis, MO), 1:1000 phosphatase inhibitor (Sigma), and 1% Triton X) and incubated on ice for 15 min. Four hundred micrograms of protein was incubated with anti-Myc (9E10) antibody for 1 hr at 4°C. Immune complexes were collected by adding 50 μl of 50% protein G-Sepharose bead slurry (GE Healthcare, Milwaukee, WI) for 1 hr at 4°C, washed three times with RIPA buffer, and then boiled in 2 × SDS buffer. The samples were resolved in 5–20% gradient polyacrylamide gels, transferred to nitrocellulose membranes and probed with antiphospho-c-Raf (S259) and anti-Myc (9E10) antibodies.

Reporter Assay

NIH 3T3 cells (ATCC) were maintained in DMEM containing 10% newborn calf serum, 50 U/ml penicillin, and 50 μg/ml of streptomycin. One day prior to the transfection, the NIH 3T3 cells were plated in 12-well plates with a density of 1×10^5 cells per well. Cells were transiently transfected using Lipofectamine and PLUS Reagents with 700 ng of pFR-luc, 15 ng of pFA2-Elk1, 7 ng of phRLnull-luc, and 35 ng of WT or mutant expression constructs of *RAF1*. Eighteen hours after transfection, the cells were cultured in DMEM without serum for 24 hr. Cells were harvested in passive lysis buffer, and luciferase activity was assayed using a Dual-Luciferase Reporter Assay System (Promega, Madison, WI). Renilla luciferase expressed by phRLnull-luc was used to normalize the transfection efficiency. The experiments were performed in triplicate. Data are shown as mean ± SD. Statistical analysis was performed using Excel.

Binding of RAF1 with 14-3-3

An expression construct containing Myc- and Flag-tagged 14-3-3 ζ (pCMV6-14-3-3 ζ) was purchased from Origene (Rockville, MD). In order to remove the Myc-tag from the construct, the 3′ half of the cDNA and the Myc-tag were removed by digestion with *Eco*RV and the 3′ half of cDNA was filled using PCR. An S621A mutation, which impairs phosphorylation of S621 to bind 14-3-3, was introduced into pUSE RAF1 harboring WT, p.S257L, or p.N262K cDNA by a Quickchange Site-Directed Mutagenesis Kit. HEK293 cells (ATCC) were transfected with 2 μg RAF1 constructs and 2 μg pCMV6-14-3-3 ζ construct using Lipofectamine and PLUS Reagents. After 48 hr, cells were scraped and collected by centrifugation after two washes with PBS. Lysates were prepared as described above. The Myc-tagged RAF1 was immunoprecipitated with anti-Myc antibody (clone4A6, Millipore) for 1 hr at 4°C. Immune complexes were collected by adding 50 μl of 50% protein G-Sepharose bead slurry (GE Healthcare) for 1 hr at 4°C, washed three times with RIPA buffer, and then boiled in 2 × SDS buffer. The samples were resolved in 5–20% gradient polyacrylamide gels, transferred to nitrocellulose membranes, and probed with anti-FLAG M2 (Sigma) and anti-Myc antibodies. For immunoprecipitation of 14-3-3, anti-FLAG M2 antibody was used and immunoblotting was performed using anti-FLAG M2 and anti-c-Raf (Cell Signaling) antibodies.

Results

Mutation Analysis in Patients

We identified eight amino acid changes in 18 patients (Table 1). A C-to-T nucleotide change, resulting in an amino acid change p.S257L, was identified in 11 patients. Novel p.R191I (c.572G>T) and p.N262K (c.786T>A) were identified in one each patient. Previously reported mutations, including p.S259F (c.776C>T), p.P261A (c.781C>G), p.P261L (c.782C>T), p.S427G (c.1279A>G), and p.L613V (c.1837C>G), were identified in a single patient. Nucleotide numbering reflects cDNA numbering with +1 corresponding to the A of the ATG translation initiation codon in Genbank NM_002880.3, according to journal guidelines (www.hgvs.org/mutnomen). The initiation codon is codon 1. The mutation p.S427G, which has been reported in a patient with therapy-related acute myeloid leukemia [Zebisch et al., 2006], was identified in one patient. None of the newly identified mutations were observed in the control DNA of 105 ethnically matched healthy subjects. Parental samples were obtained from six patients (NS86, 92, 209, 210, 222, and 258). The analysis showed that p.S257L, p.P261A, and p.N262K occurred de novo. p.S427G was also identified as well in his 32-year-old mother, who also exhibited a Noonan phenotype with distinctive facial appearance, sparse hair in infancy, and multiple lentigines. The p.H103Q (c.309C>G) was identified in patient NS86, in whom p.S257L was also identified. This amino acid change was identified in one of his parents without any clinical features, suggesting that this amino acid change was polymorphic.

Clinical Manifestations of Patients with *RAF1* Mutations

Initial diagnoses of patients with *RAF1* mutations were as follows: NS in 11 patients, CFC syndrome in 4 patients, and Costello in 3 patients (Supp. Table S2). Four patients who were first diagnosed as having CFC syndrome were reclassified as NS because of facial features and normal mental development after identification of *RAF1* mutations. Three patients were diagnosed as having Costello syndrome. One patient was rediagnosed as having NS (NS135) and the other patient died at 1 month (NS209). Detailed information on clinical manifestations of NS205 was not available.

Detailed clinical manifestations in 18 patients with *RAF1* mutations were evaluated (Table 2 and Fig. 1). Nine of 15 patients had prenatal abnormality, including cystic hygroma, polyhydramnions, and asphyxia. Most patients had characteristic craniofacial abnormalities frequently observed in NS: relative macrocephaly (94%), hypertelorism (93%), downslanting palpebral fissures (63%), epicanthal folds (86%), and low-set ears (93%). Mental retardation was observed in 6 of 11 (55%) patients. Short stature (73%), short neck (93%), and webbing of neck (81%) were also observed. As for cardiac abnormalities, hypertrophic cardiomyopathy was observed in 10 of 16 patients (63%), followed by pulmonic stenosis (47%),

Table 1. *RAF1* Mutations Identified in This Study*

Patient ID	Country of origin	Final diagnosis	Exon	Nucleotide change	Amino acid change	Domain	Genotype of father/mother
NS213	France	atypical NS	5	c. 572G>T	p.R191I[a]	CR1	NA
NS39	Japan	NS	7	c.770C>T	p.S257L	CR2	NA
NS86	France	NS	3, 7	c.309C>G	p.H103Q	CR1,	H103Q/WT
				c.770C>T	p. S257L	CR2	WT/WT
NS92	Germany	NS	7	c.770C>T	p.S257L	CR2	WT/WT
NS135	Japan	NS	7	c.770C>T	p.S257L	CR2	NA
NS146	Spain	NS	7	c.770C>T	p.S257L	CR2	NA
NS199	Japan	NS	7	c.770C>T	p.S257L	CR2	NA
NS200	France	NS	7	c.770C>T	p.S257L	CR2	NA
NS215	Japan	NS	7	c.770C>T	p.S257L	CR2	NA
NS227	Japan	NS	7	c.770C>T	p.S257L	CR2	NA
NS256	Japan	NS	7	c.770C>T	p.S257L	CR2	NA
NS258	Japan	NS	7	c.770C>T	p.S257L	CR2	WT/WT
NS279	Japan	NS	7	c.776C>T	p.S259F	CR2	NA
NS210	France	NS	7	c.781C>G	p.P261A	CR2	WT/WT
NS205	France	CS[b]	7	c.782C>T	p.P261L	CR2	NA
NS209	France	CS[c]	7	c.786T>A	p.N262K[a]	CR2	WT/WT
NS222	Japan	NS	12	c.1279A>G	p.S427G[d]	CR3	WT/p.S427G
NS285	Japan	NS	17	c.1837C>G	p.L613V	CR3	NA

NS, Noonan syndrome; CS, Costello syndrome; WT, wild type; CR, conserved region; NA, not available.
*GenBank RefSeq: NM_002880.3 Nucleotide numbering reflects cDNA numbering with +1 corresponding to the A of the ATG translation initiation codon in the reference sequence, according to journal guidelines (www.hgvs.org/mutnomen). The initiation codon is codon 1.
[a]Novel mutation.
[b]Detailed clinical manifestations were not obtained.
[c]The patient died at 1 month.
[d]The mutation was previously identified in a patient with a therapy-related acute leukemia.

ASD (31%), arrhythmia (38%), and mitral valve anomaly (29%). Other observed clinical features were hyperelastic skin (58%), curly hair (47%), and cryptorchidism in males (50%). Coagulation defects were observed in two patients.

Four patients with *RAF1* mutations died before 5 years of age (Supp. Table S2). Patient NS39 were diagnosed as having cystic hygroma in the prenatal period and had suffered from neonatal hypertrophic cardiomyopathy. At 1 year of age, she contracted acute respiratory distress syndrome after having pneumonia and died of respiratory failure. Patient NS199 had been suspected to have achondroplasia because of short limbs. He was diagnosed as having NS at 3 years of age because of distinct facial features, growth failure, short stature, and hypertrophic cardiomyopathy. He had pneumonia without fever for a week and died suddenly at 5 years of age. Patient NS227 suffered from feeding difficulties, ectopic atrial tachycardia, as well as VSD and pulmonary hypertension. The patient died at 2 months of tachycardia (>200/min) and laryngeal edema.

Clinical manifestations in our patients with *RAF1* mutations were compared with those previously reported (Table 2). The high frequency of hypertrophic cardiomyopathy in our study (63%) was consistent with that observed in patients with *RAF1* mutations previously reported (77%). The frequency of ASD and that of mitral valve anomaly were similar to those of the previous studies. However, the frequency of PS in our study (47%) was higher than that previously reported (11%). Arrhythmia was less frequently observed in our patients with *RAF1* mutations (38 vs. 89%). The frequency of mental retardation (55%) was almost same as that of the previous studies (56%). Hyperelastic skin (58%) and coagulation defects (two cases) were also described in previously reported patients with *RAF1* mutations (24% and one case, respectively).

Phosphorylation State of Mutant RAF1 Proteins

RAF1 is a ubiquitously expressed RAF serine/threonine kinase, which regulates the RAS pathway. It has been shown that phosphorylation of serine, threonine, and tyrosine residues contributes to a conformational change of RAF1 protein and activation in growth factor stimulation [Mercer and Pritchard, 2003]. In the inactive state, phosphorylated S259 and S621 serve as binding sites for 14-3-3, leading to a closed confirmation [Dhillon et al., 2007]. Phosphorylation of S621 seems essential for RAF1 activation. In contrast, phosphorylation of serine 259 has been shown to have an inhibitory role in RAF1 activation. When cells are stimulated with growth factors, dephosphorylation of S259 by protein phosphatase 1 (PP1) and/or protein phosphatase 2A (PP2A) promotes the dissociation of 14-3-3 from RAF1, resulting in an activated conformation of RAF1 protein. For full activation, multiple residues, including S338, are phosphorylated and substrate of RAF1 enters the catalytic cleft in the CR3 kinase domain. Negative feedback from activated ERK results in the phosphorylation of S289, 296, and 301 [Dhillon et al., 2007].

To examine the phosphoryalation status of mutants observed in NS patients, we transfected constructs harboring WT *RAF1* cDNA and five mutants identified in NS patients. Immunoblotting was performed using four phospho-specific antibodies of RAF1 (Fig. 2A). We first analyzed the phosphorylation status of two phosphorylation sites, S259 and S621, using antibodies that recognize each site. Immunoblotting showed that phosphorylation of S259 was scarcely observed in cell lysates expressing p.S257L and p.N262K. In contrast, phosphorylation of S259 of p.H103Q, p.R191I, and p.S427G was similar to that in WT RAF1. To confirm this observation, immunoprecipitation was performed using an anti-Myc antibody, and phosphorylation levels at S259 were examined (Fig. 2B). Immunoprecipitated RAF1 mutants (p.S257L and p.N262K) were not phosphorylated at S259, confirming that these mutants had impaired phosphorylation of S259. The phosphorylation level of S621 in four mutants (p.H103Q, p.R191I, p.S257L, and p.N262K) was similar to that in WT (Fig. 2A), whereas that in cells expressing p.S427G was enhanced. Phosphorylation levels at S338 and S289/296/301 were similar to that in WT except for p.S427G (Fig. 2A).

Phosphorylation levels at S259, S289/296/301, S338, and S621 were shown to be enhanced in cells expressing p.S427G. The expression of p.S427G appeared enhanced and the band was

Table 2. Clinical Manifestations in *RAF1*-Positive Patients in This Study and Past Studies

	Present cohort (%)	NS with *RAF1* mutations (%)	LS with *RAF1* mutations (%)
Number of patients in total	17	35[a]	2
Perinatal abnormality			
Polyhydramnios	6/15 (40)	6/19 (32)	ND
Fetal macrosomia	5/11 (45)	6/20 (30)	ND
Growth and development			
Failure to thrive in infancy	10/12(83)	3	ND
Mental retardation	6/11 (55)	19/34 (56)	1
Outcome			
Died	4/17 (24)	2/11 (18)	ND
Craniofacial characteristics			
Relative macrocephaly	16/17 (94)	16/21 (76)	ND
Hypertelorism	14/15 (93)	20/21 (95)	2
Downslanting palpebral fissures	10/16 (63)	19/21 (90)	2
Ptosis	9/16 (56)	19/21 (90)	1
Epicanthal folds	12/14 (86)	12/21 (57)	1
Low-set ears	14/15 (93)	18/21 (86)	2
Skeletal characteristics			
Short stature	11/15 (73)	30/35 (86)	2
Short neck	14/15 (93)	21/31 (68)	2
Webbing of neck	13/16 (81)	25/30 (83)	2
Cardiac defects			
Hypertrophic cardiomyopathy	10/16 (63)	27/35 (77)	2
Atrial septal defect	5/16 (31)	11/35 (31)	0
Ventricular septal defect	3/17 (18)	3/35 (9)	0
Pulmonic stenosis	7/15 (47)	4/35 (11)	1
Patent ductus arteriosus	2/17 (12)	ND	ND
Mitral valve anomaly	5/17 (29)	8/32 (25)	2
Arrhythmia	6/16 (38)	8/9 (89)	ND
Others	TR 1, PH 1, atrioventricular valve dysplasia 1, valvular AS 1	polyvalvular dysplasia 2 pulmonary valve dysplasia 1, PFO 1, TOF 2, AS 1, right shaft deflection 1	
Skeletal/extremity deformity			
Cubitus valgus	2/9 (22)	7/22 (32)	2
Pectus deformity	5/13 (38)	20/31 (65)	2
Others		prominent finger pads 2	prominent finger pads 1
Skin/hair anomaly			
Curly hair	8/17 (47)	6/24 (25)	2
Hyperelastic skin	7/12 (58)	5/21 (24)	2
Café au lait spots	1/14 (7)	2/20 (10)	2
Lentigines	1/14 (7)	2/21 (10)	2
Naevus	3/15 (20)	9/22 (41)	0
Others	low posterior implantation 4, hyperpigmentation 3, redundant skin 3, sparse hair 2, sparse eyebrows 2, hemangioma 2	dry skin 3, sparse hair 3, sparse eyebrows 2, keratosis pilaris 2	
Genitalia	6/11 (55)	11/16 (69)	
Cryptorchidism	5/10 (50)	8/13 (62)	ND
Blood test abnormality			
Coagulation defects	2/11 (18)	1/4 (25)	ND

NS, Noonan syndrome; LS, LEOPARD syndrome; ND, not described; TR, tricuspid regurgitation; PH, pulmonary hypertension; AS, aortic stenosis; PFO, patent foramen ovale; TOF, tetralogy of Fallot.

[a]Includes affected family members. Clinical manifestations in 3, 21, and 11 NS patients with *RAF1* mutations were summarized from three reports [Ko et al., 2008; Pandit et al., 2007; Razzaque et al., 2007], respectively.

rather broad. However, Western blotting using antineomycin phosphoacetyltransferase antibody that recognizes the amount of plasmids introduced in cells showed that the transfection efficiency in cells expressing p.S427G was similar to that in cells expressing other mutants (Fig. 2A). These findings were consistently observed in three independent experiments. Recent studies have shown that autophosphorylation of S621 is required to prevent proteasome-mediated degradation [Noble et al., 2008]. To explore the possibility that p.S427G mutant is resistant to proteasome-mediated degradation, we examined the amount of WT RAF1 and p.S427G at 24, 48, and 72 hr after transfection in serum-starved or complete medium (Fig. 2C). The results showed that the expression of Myc-tagged RAF1 in cells expressing p.S427G was similar to that in WT RAF1, although multiple bands were observed, suggesting the hyperphosphorylation of the p.S427G mutant.

ELK Transactivation in Mutant RAF1 Proteins

To examine the effect on the downstream pathway of mutant RAF1, we introduced five RAF1 mutants into NIH3T3 cells and examined ELK transactivation (Fig. 2D). ELK is a transcription factor, which is phosphorylated by activated ERK and then binds the serum response element in the promoter of the immediate-early genes, including *C-FOS*. ELK transactivation was enhanced in cells expressing p.S257L, p.N262K, and p.S427G without any stimulation, suggesting that these mutants were gain-of-function

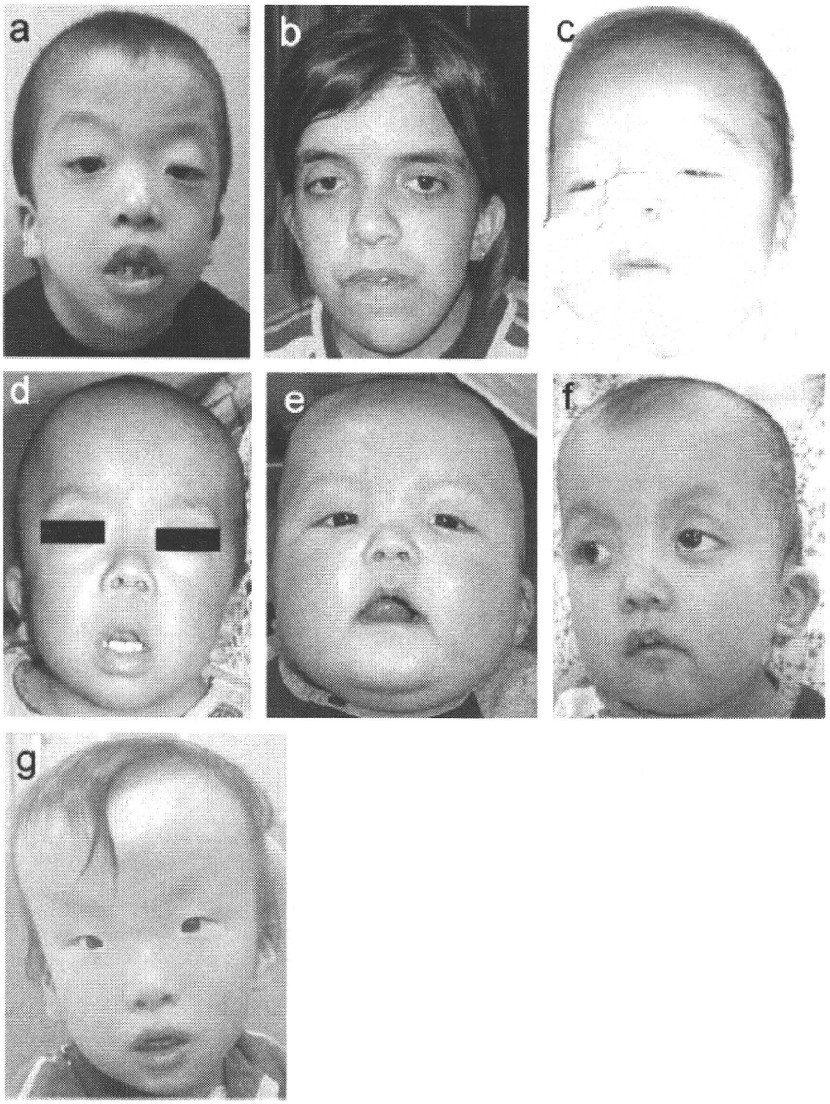

Figure 1. Facial appearance of patients with *RAF1* mutations. **a–f:** patients with p.S257L mutations. **a:** NS135; **b:** NS146; **c:** NS215; **d:** NS256; **e:** NS258 at 6 months; **f:** 2 years and 4 months; **g:** NS222 with p.S427G. [Color figure can be viewed in the online issue, which is available at www.interscience.wiley.com.]

mutations. ELK transactivation in cells expressing p.H103G and p.R191I was not enhanced.

Phosphorylation State, ERK Activation, and Binding to the Scaffolding Protein 14-3-3 in Mutations in the CR2 Domain

Previous studies as well as the present study showed that mutations in NS-associated *RAF1* mutations were clustered in the CR2 domain. We hypothesized that amino acid changes in the CR2 domain impaired phosphorylation of serine at 259. We additionally generated expression construct harboring p.S259F and p.P261A substitutions, and their phosphorylation status was examined using anti-pRAF1 (S259) antibody together with RAF1 WT, p.S257L, p.N262K, and p.S427G (Fig. 3A). The results showed that phosphorylated proteins were scarcely observed in p.S257L, p.S259F, p.P261A, and p.N262K. Phosphorylation of ERK p44/42 was determined using anti-p-ERK (p44/42) antibody. All mutations activated the downstream ERK without any stimulation. The level of ERK phosphorylation in cells expressing mutants was lower than that in those treated with epidermal growth factor (EGF), suggesting that the expression of p.S257L, p.S259F, p.P261A, and p.N262K resulted in a partial activation of ERK.

Anti-pRAF1 (S259) antibody was produced by immunizing rabbits with a synthetic phospho-peptide corresponding to residues surrounding Ser259 of human RAF1. To examine if this antibody was able to recognize phosphorylation at S259 when mutations such as S257L and N262K were introduced, we performed a solid-phase immunoassay using biotinylated peptides as per the manufacturer's recommendation (Mimotopes, Victoria, Australia; Supp. Methods). The result showed that at least in peptides, this antibody could recognize serine phosphorylation in amino acid 259 when mutations S257L and N262K were introduced (Fig. 3B). These results support the data in Figure 3A, suggesting that S259 was not phosphorylated in mutants in the CR2 domain.

To examine if the RAF1 mutants without S259 phosphorylation were able to bind to 14-3-3, we cotransfected three double mutants (WT/S621A, S257L/S621A, and N262K/S621A) with FLAG-tagged 14-3-3, and coimmunoprecipitation was performed using anti-Myc antibody (Fig. 3C). The result showed that the WT/S621A mutant bound 14-3-3. In contrast, p.S257L/S621A and

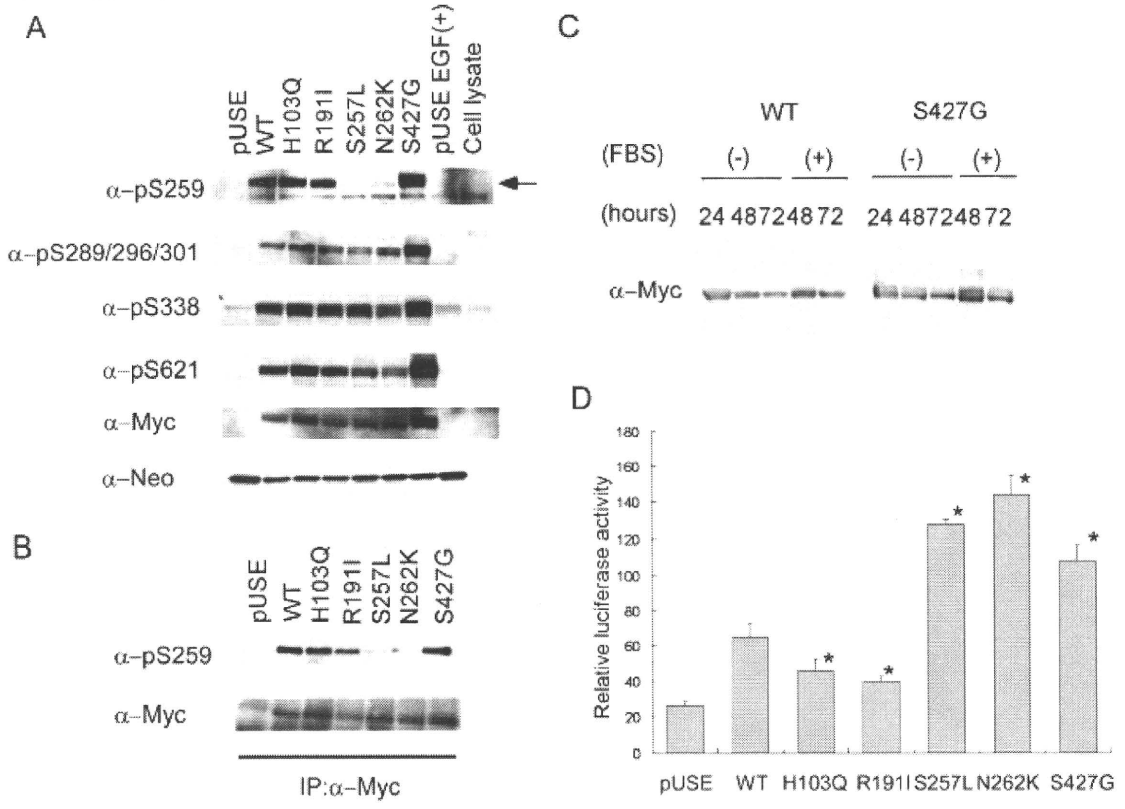

Figure 2. Analysis of phosphorylation status, degradation, and effect on downstream signaling in RAF1 mutants identified in this study. **A:** Phosphorylation status of wild-type (WT) RAF1 and mutants. Expression levels of RAF1 proteins and their phosphorylation levels were detected with different antibodies indicated in the figure. Transfection efficiency was measured using antineomycin phosphotransferase II (α-Neo) antibody. The arrow indicates the serine-phosphorylated expressed RAF1. **B:** Phosphorylation of S259 was confirmed by immunoprecipitation. Myc-tagged RAF1 was immunoprecipitated using anti-Myc antibody and the phosphorylation of S259 was determined. **C:** Time course experiments of WT RAF1 and p.S427G. The RAF1 protein was detected using anti-Myc antibody (clone 4A6; Millipore). FBS, fetal bovine serum. **D:** ELK transactivation in WT and mutants. Results are expressed as the means and standard deviations of mean values from triplicate samples. A significant increase in relative luciferase activity (RLA) was observed in cells transfected with p.S257L, p. N262K, and p.S427G, but not in cells transfected with p.H103Q or p.R191I. WT, wild-type; $^*P<0.01$ by Student's *t*-test.

p.N262K/S621A mutants did not bind 14-3-3, suggesting that the decreased phosphorylation of S259 prevented 14-3-3 binding. A similar result was obtained in the coimmunoprecipitation study using anti-FLAG antibody (Fig. 3D). These results showed that mutants in the CR2 domain impaired phosphorylation of S259, abrogated the binding to 14-3-3 and resulted in a partial activation of ERK.

Discussion

In this study, we identified eight different *RAF1* mutations in 18 patients: p.S257L in 11 patients and p.R191I, p.S259F, p.P261A, p.P261L, p.N262K, p.S427G, and p.L613V in one patient each. Sixteen patients were diagnosed as having NS, although we were not able to reevaluate 2 patients with Costello syndrome. Examination of detailed clinical manifestations in the present study and past studies showed that patients with *RAF1* mutations were associated with hypertrophic cardiomyopathy, arrhythmia, and mental retardation. Results from previous studies and the present study showed 41/52 (79%) mutations to be located in the CR2 domain (Fig. 3E). We first demonstrated that mutations in the CR2 domain had impaired phosphorylation of S259. This caused the impaired binding of RAF1 to 14-3-3, resulting in a partial activation of downstream ERK. These results suggest that dephosphorylation of S259 is the primary mechanism of activation of mutant RAF1 located in the CR2 domain.

Phosphorylation of S259 and subsequent binding to 14-3-3 have been shown to be important for suppression of RAF1 activity [Dhillon et al., 2007]. Light et al. [2002] examined the phosphorylation status at S259 in the p.S257L mutant. Their experiment showed that phosphorylation of S259 still existed in the p.S257L mutant. The mutant was not able to bind 14-3-3 [Light et al., 2002]. In contrast, our functional studies demonstrated that all four mutants located in the CR2 domain (p.S257L, p.S259F, p.P261A, and p.N262K) impaired phosphorylation of S259 and that two of them impaired binding of 14-3-3. Impaired binding to 14-3-3 was also shown in p.P261S mutant [Pandit et al., 2007]. The reason for the difference on S259 phosphorylation between the result by Light et al. [2002] and ours is unclear. Enhanced kinase activities of mutants, including p.S257L, p.P261S, p.P261A, and p.V263A, were demonstrated in a previous study [Razzaque et al., 2007]. Phosphorylation levels at S338 in p.S257L and p.N262K were not enhanced compared to that in WT RAF1 (Fig. 2A), suggesting that the activation mechanism in these mutants is different from that of the normal state upon RAS-GTP binding. Indeed, ERK activation was partial compared with that in cells after EGF treatment (Fig. 3A). These results suggest that the conformational change around S259 due to amino acid changes results in the decreased phosphorylation of S259 and that mutant

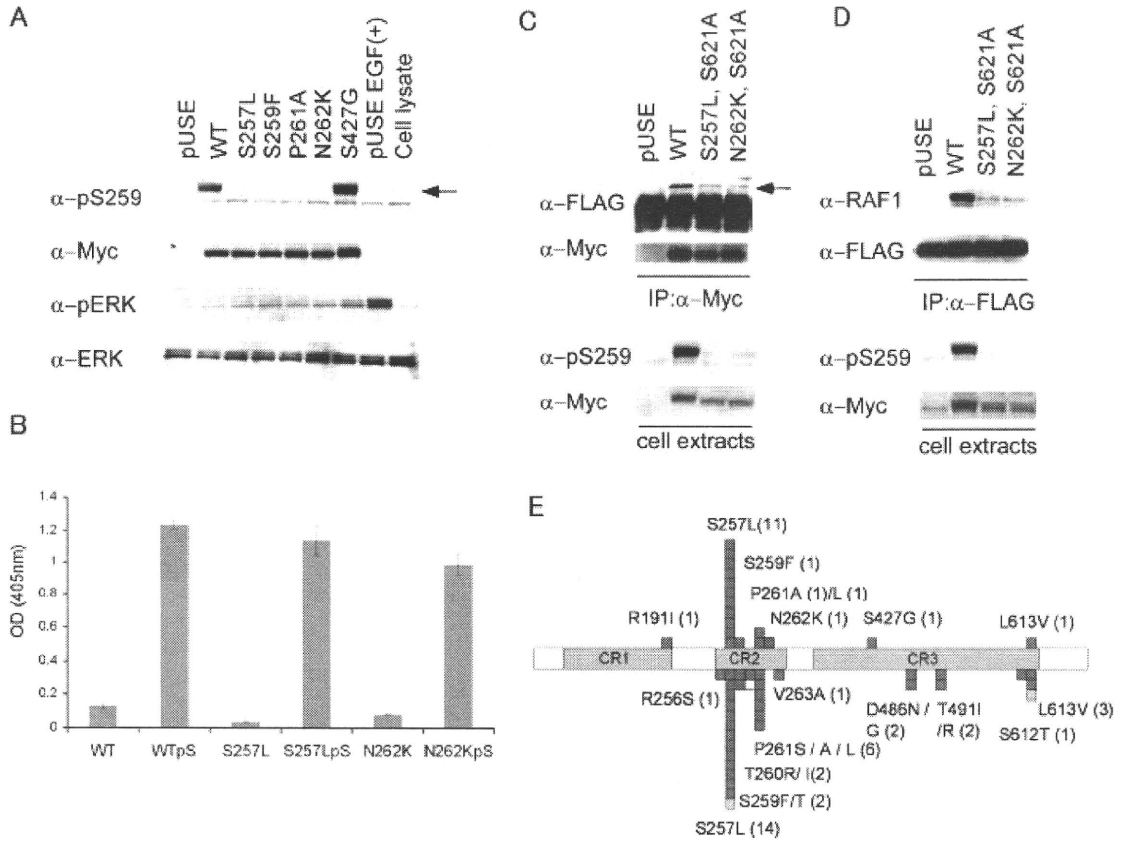

Figure 3. Phosphorylation of S259, binding to 14-3-3 and ERK activation of mutants located in the CR2 domain. **A:** Phosphorylation status of WT and mutants located in the CR2 domain. Phosphorylation of S259 was not observed in cells expressing p.S257L, p.S259F, p.P261A, and p.N262K. In order to examine the level of full activation of ERK, mock-transfected cells were treated with 10 ng/ml EGF. ERK activation was observed in cells expressing p.S257L, p.S259F, p.P261A, and p.N262K, but was weaker than those in cells expressing p.S427G and EGF-treated cells. The arrow indicates the serine-phosphorylated expressed RAF1. **B:** Epitope mapping of the anti-pRAF1 (S259) antibody using a solid-phase immunoassay. The antibody was able to recognize peptides with S257L or N262K mutations when S259 was phosphorylated, but was not able to recognize peptides without Ser259 phosphorylation. Results are expressed as the means and standard deviations of mean values from triplicate samples. **C:** Binding of RAF-1 to 14-3-3ζ. HEK293 cells were transfected with constructs harboring FLAG-tagged 14-3-3 and one construct of pUSE WT, p.S257L/p.S621A, or p.N262K/ p.S621A. Immunoprecipitation was performed using anti-Myc antibody, and 14-3-3 binding was determined by anti-FLAG antibody (upper panel). Phosphorylation of S259 and RAF1 expression were determined in cell lysates used for the immunoprecipitation (lower panel). The arrow indicates the band for 14-3-3. **D:** Binding of 14-3-3ζ to RAF-1. Immunoprecipitation was performed using anti-FLAG antibody and RAF1 binding was examined using anti-RAF1 antibody (upper panel). The binding of 14-3-3 to endogenous RAF1 was scarcely observed (lane 1, pUSE). Phosphorylation of S259 and RAF1 expression were determined using cell lysates used for the immunoprecipitation (lower panel). **E:** Domain organization and the distribution of mutations in RAF1 protein. The three regions conserved in all RAF proteins (conserved region [CR] 1, CR2, and CR3) are shown in pink. Mutations identified in this study are shown above the bar and those reported before [Ko et al. 2008; Pandit et al. 2007; Razzaque et al. 2007] are shown below the bar. Green squares indicate families with NS. Orange squares indicate patients with LEOPARD syndrome and the yellow square indicates a patient with hypertrophic cardiomyopathy.

RAF-1 then dissociates from 14-3-3; the substrate would thus be targeted to the catalytic domain in the CR3 domain (Fig. 4).

To highlight the clinical pictures of patients with *RAF1* mutations, clinical manifestations in 52 patients with *RAF1* mutations [Ko et al., 2008; Pandit et al., 2007; Razzaque et al., 2007], 172 patients with *PTPN11* mutations [Jongmans et al., 2005; Musante et al., 2003; Tartaglia et al., 2002; Zenker et al., 2004], 73 patients with *SOS1* mutations [Ferrero et al., 2008; Narumi et al., 2008; Roberts et al., 2007; Tartaglia et al., 2007; Zenker et al., 2007a] and 18 patients with *KRAS* mutations [Carta et al., 2006; Ko et al., 2008; Lo et al., 2008; Schubbert et al., 2006; Zenker et al., 2007b] are summarized in Table 3. The frequency of perinatal abnormalities was similar between patients with *RAF1* and *SOS1*. In contrast, the description of perinatal abnormalities was rare in patients with *PTPN11* and *KRAS* mutations. Growth failure and mental retardation were observed in 100 and 94% of NS with *KRAS* mutations, respectively. Growth failure and mental retardation were observed in 87 and 56% of patients with *RAF1* mutations, respectively. In contrast, those manifestations were less frequent (63 and 43%) in patients with *PTPN11* mutations. The frequency of mental retardation was lowest in patients with *SOS1* mutations (18%). We were unable to compare gene-specific features in craniofacial characteristics because such details were not described in the previous reports. As for skeletal characteristics, short stature was frequently manifested in patients with *RAF1* mutations (82%) followed by *KRAS* mutation-positive patients (71%). The association of short stature was lower in *PTPN11* mutation-positive and *SOS1* mutation-positive patients (56 and 38%, respectively). It is noteworthy that the association of hypertrophic cardiomyopathy was specifically high (73%) in *RAF1* mutation-positive patients. In contrast, hypertrophic cardiomyopathy was observed in 20% of clinically diagnosed Noonan

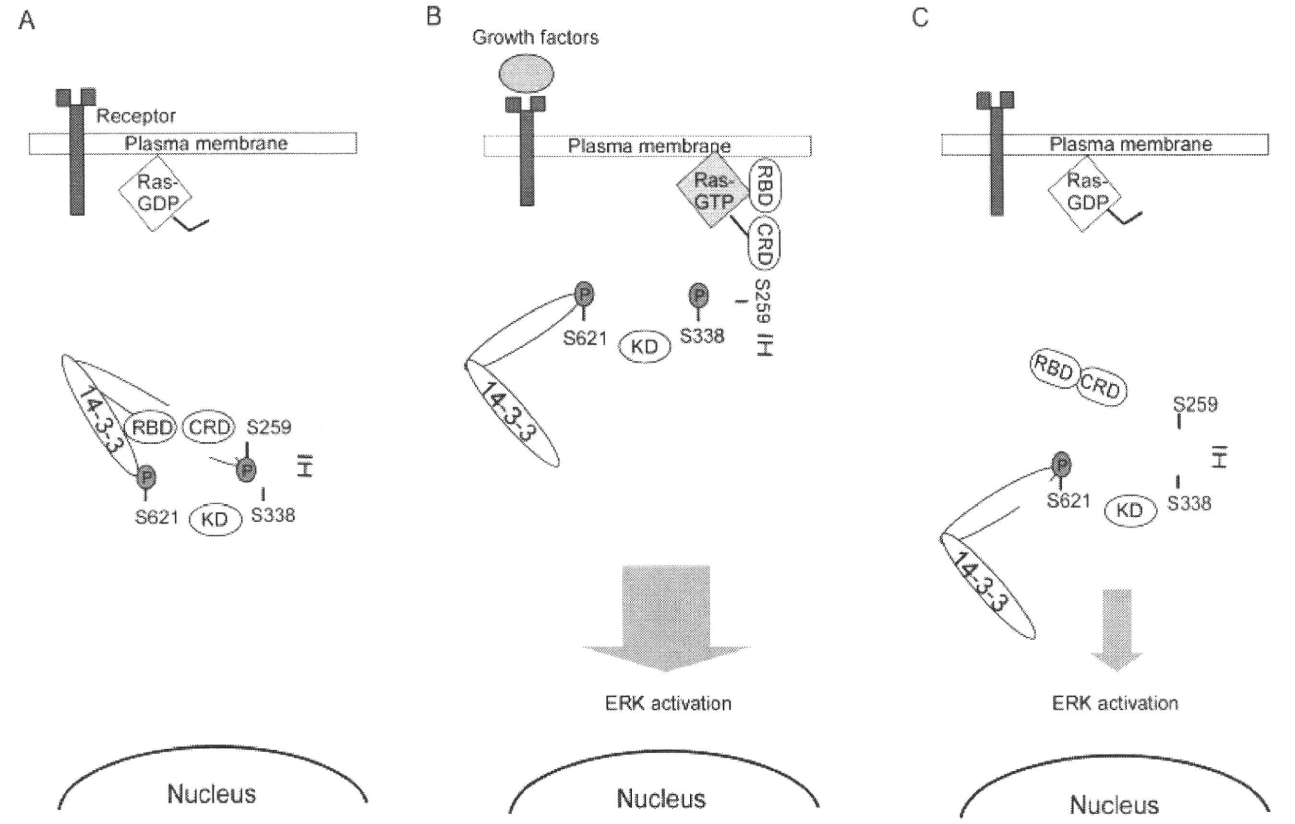

Figure 4. Schematic model of WT and mutant activation. **A:** In an inactive state, RAF1 is phosphorylated on S259 and S621 and is bound to 14-3-3. **B:** In growth-factor stimulation, the GTP-bound RAS binds to the CR1 domain of RAF1, which displaces 14-3-3. S259 is dephosphorylated by protein phosphatase 1 (PP1) and/or protein phosphatase 2A (PP2A). After RAF1 is recruited to the plasma membrane, phosphorylation of S338, Y341, T491, and S494 occurs. The phosphorylation of these residues is thought to be important for the full activation of RAF1. **C:** Mutants whose amino acid changes are located in the CR2 domain. It has been reported that S259 was phosphorylated by Akt and dephosphorylated by PP1 and/or PP2A. Amino acid changes in the CR2 domain would cause structural changes in the CR2 domain, leading to the access of PP2A to S259. Alternatively, Akt kinase would not be able to phosphorylate S259. S259 is dephosphorylated without stimulation and substrate(s) would be able to enter the kinase domain, leading to a partial activation. RBD, RAS-binding domain; CRD, cysteine-rich domain; KD, kinase domain; IH, isoform-specific hinge segment region. [Color figure can be viewed in the online issue, which is available at www.interscience.wiley.com.]

patients [van der Burgt 2007] and in 7, 10, and 17% of patients with *PTPN11*, *SOS1*, and *KRAS* mutations, respectively. These results strongly suggest that patients with *RAF1* mutations have a significantly higher risk of hypertrophic cardiomyopathy. Mitral valve abnormality and arrhythmia were also frequently observed in patients with *RAF1* mutations (27 and 56%, respectively). In summary, these results highlight specific manifestations of patients with *RAF1* mutations: high frequency of hypertrophic cardiomyopathy, septal defects of the heart, short stature, and less frequent PS (Supp. Fig. S1). The high frequency of heart defects would be associated with a high risk of sudden death in *RAF1* mutation-positive patients.

The present study is the first to identify p.S427G in a patient with NS. The same mutation has been reported in a patient with therapy-related acute myeloid leukemia [Zebisch et al., 2006]. The patient reported by Zebisch et al. [2006] first developed immature teratoma, yolk sack tumor, and embryonal testicular carcinoma. Thirty-five months after tumor resection and chemotherapy, the patient developed acute myeloid leukemia. Molecular analysis of *RAF1* revealed the de novo p.S427G mutation in leukemia cells and DNA from buccal epithelial cells [Zebisch et al., 2006]. Whether or not the patient had an NS phenotype was not mentioned. *RAF1* mutations have been rarely reported in malignant tumors. As far as we could determine, only six mutations, including p.P207S, p.V226I, p.Q335H, p.S427G, p.I448V, and p.E478K, have been identified in tumors and therapy-related leukemias [Pandit et al., 2007; Razzaque et al., 2007]. A previous study as well as our results showed that p.S427G mutant has transformation capacity [Zebisch et al., 2009], is resistant to apoptosis when introduced into NIH3T3 cells [Zebisch et al., 2009] and activates ERK and ELK transcription, suggesting that p.S427G is a gain-of-function mutation. We identified p.S427G in a familial case of NS. The mother and boy have not yet developed malignant tumors. Although no NS patients with *RAF1* mutations have developed malignant tumors, careful observation might be prudent in *RAF1* mutation-positive children.

We identified two novel mutations, p.R191I and p.N262K. p.R191I is located in the CR1, and arginine at amino acid position 191 is evolutionally conserved [Mercer and Pritchard, 2003]. Activation of ERK was not observed in cells expressing p.R191I. ELK transactivation was rather decreased; parental samples were not available. There is a possibility that this change is a polymorphism.

In conclusion, we identified *RAF1* mutations in 18 patients and detailed clinical manifestations in mutation-positive patients were examined. Our analysis of patients with mutations in *RAF1*, *PTPN11*, *SOS1*, and *KRAS* showed hypertrophic cardiomyopathy and short stature to be frequently observed in patients with *RAF1* mutations. Functional analysis revealed that dephosphorylation of S259 would be the essential mechanism for ERK activation in RAF1 mutations. Despite recent progress in molecular characterization of NS and related disorders, genetic causes in

Table 3. Clinical Manifestations in NS Patients with *RAF1, PTPN11, SOS1,* and *KRAS* Mutations

	RAF1[a] (%)	PTPN11[b] (%)	SOS1[c] (%)	KRAS[d] (%)
Total patients	52	172	73	18
Perinatal abnormality				
Polyhydramnios	12/34 (35)	ND	9/16 (56)	2
Fetal macrosomia	11/31 (35)	ND	9/15 (60)	ND
Growth and development				
Failure to thrive in infancy	13/15 (87)	35/56 (63)	ND	3/3 (100)
Mental retardation	25/45 (56)	71/164 (43)	12/67 (18)[e]	16/17 (94)[f]
Outcome				
Died	6/28 (21)	ND	ND	ND
Craniofacial characteristics				
Relative macrocephaly	32/38 (84)	ND	9/21 (43)[e]	9/11 (82)
Hypertelorism	34/36 (94)	15/28 (54)[e]	5/6 (83)	12/12 (100)
Downslanting palpebral fissures	29/37 (78)	19/28 (68)	20/22 (91)	9/12 (75)
Ptosis	28/37 (76)	18/29 (62)	19/24 (79)	10/15 (67)
Epicanthal folds	24/35 (69)	15/28 (54)	ND	2/9 (22)[e]
Low set ears	32/36 (89)	56/64 (88)	20/22 (91)	7/10 (70)
Skeletal characteristics				
Short stature	41/50 (82)	97/172 (56)[e]	22/58 (38)[e]	12/17 (71)
Short neck	35/46 (76)	15/29 (52)[e]	17/22 (77)	9/10 (90)
Webbing of neck	38/46 (83)	36/122 (30)[e]	3/6 (50)	7/14 (50)[e]
Cardiac defects				
Hypertrophic cardiomyopathy	37/51 (73)	10/135 (7)[e]	7/73 (10)[e]	3/18 (17)[e]
Septal defect	22/52 (42)	41/170 (24)[e]	17/73 (23)[e]	5/18 (28)
Atrial septal defect	16/51 (31)			4/18 (22)
Ventricular septal defect	6/52 (12)			1/18 (6)
Pulmonic stenosis	11/50 (22)	125/171 (73)[f]	53/73 (73)[f]	7/18 (39)
Patent ductus arteriosus	2/20 (10)	ND	ND	1/18 (6)
Mitral valve anomaly	13/49 (27)	ND	ND	3/18 (17)
Arrhythmia	14/25 (56)	ND	ND	ND
Skeletal/extremity deformity				
Cubitus valgus	9/31(29)	14/61 (23)	1/6 (17)	2/2 (100)
Pectus deformity	25/44 (57)	108/171 (63)	38/56 (68)	13/16 (81)
Skin/hair anomaly				
Curly hair	14/41 (34)	ND	15/22 (68)[f]	1/12 (8)
Hyperelastic skin	12/33 (36)	ND	1/6 (17)	3/12 (25)
Café au lait spots	3/34 (9)	ND	1/6 (17)	1/9 (11)
Lentigines	3/35 (9)	ND	ND	ND
Naevus	12/37 (32)	ND	ND	ND
Genitalia				
Cryptorchidism	13/23 (57)	75/138 (54)	22/39 (56)	4/11 (36)
Blood test abnormality				
Coagulation defects	3/15 (20)	46/90 (51)	14/66 (21)	2/9 (22)

ND, not described.
[a][Ko et al., 2008; Pandit et al., 2007; Razzaque et al., 2007]; and this study.
[b][Jongmans et al., 2005; Musante et al., 2003; Tartaglia et al., 2002; Zenker et al., 2004].
[c][Ferrero et al., 2008; Ko et al., 2008; Narumi et al., 2008; Roberts et al., 2007; Tartaglia et al., 2007; Zenker et al., 2007a].
[d][Carta et al., 2006; Ko et al., 2008; Lo et al., 2008; Schubbert et al., 2006; Zenker et al., 2007b].
[e]The frequency of the manifestation in patients with the gene was significantly lower compared with that observed in *RAF1*-positive patients ($P < 0.05$ by Fisher's exact test).
[f]The frequency of the manifestation in patients with the gene was significantly higher compared with that observed in *RAF1*-positive patients ($P < 0.05$ by Fisher's exact test).

approximately 30% of NS and related disorders remain unknown. Presently unknown genetic causes for mutation-negative NS and related disorders remain to be identified in molecules in future studies.

Acknowledgments

The authors wish to thank the patients and their families who participated in this study. We are grateful to physicians who referred the patients and to Kumi Kato and Miyuki Tsuda for technical assistance. This work was supported by Grants-in-Aids from the Ministry of Education, Culture, Sports, Science and Technology of Japan, Japan Society for the Promotion of Science, and The Ministry of Health Labour and Welfare to Y.M. and Y.A. and by an outstanding Senior Graduate Student award from Tohoku University Graduate School of Medicine to T.K.

References

Allanson JE, Hall JG, Hughes HE, Preus M, Witt RD. 1985. Noonan syndrome: the changing phenotype. Am J Med Genet 21:507–514.

Aoki Y, Niihori T, Kawame H, Kurosawa K, Ohashi H, Tanaka Y, Filocamo M, Kato K, Suzuki Y, Kure S, Matsubara Y. 2005. Germline mutations in HRAS proto-oncogene cause Costello syndrome. Nat Genet 37:1038–1040.

Aoki Y, Niihori T, Narumi Y, Kure S, Matsubara Y. 2008. The RAS/MAPK syndromes: novel roles of the RAS pathway in human genetic disorders. Hum Mutat 29:992–1006.

Bentires-Alj M, Kontaridis MI, Neel BG. 2006. Stops along the RAS pathway in human genetic disease. Nat Med 12:283–285.

Brems H, Chmara M, Sahbatou M, Denayer E, Taniguchi K, Kato R, Somers R, Messiaen L, De Schepper S, Fryns JP, Cools J, Marynen P, Thomas G, Yoshimura A, Legius E. 2007. Germline loss-of-function mutations in SPRED1 cause a neurofibromatosis 1-like phenotype. Nat Genet 39:1120–1126.

Carta C, Pantaleoni F, Bocchinfuso G, Stella L, Vasta I, Sarkozy A, Digilio C, Palleschi A, Pizzuti A, Grammatico P, Zampino G, Dallapiccola B, Gelb BD, Tartaglia M. 2006. Germline missense mutations affecting KRAS isoform B are associated with a severe Noonan syndrome phenotype. Am J Hum Genet 79:129–135.

Dhillon AS, von Kriegsheim A, Grindlay J, Kolch W. 2007. Phosphatase and feedback regulation of Raf-1 signaling. Cell Cycle 6:3–7.

Digilio MC, Conti E, Sarkozy A, Mingarelli R, Dottorini T, Marino B, Pizzuti A, Dallapiccola B. 2002. Grouping of multiple-lentigines/LEOPARD and Noonan syndromes on the PTPN11 gene. Am J Hum Genet 71:389–394.

Ferrero GB, Baldassarre G, Delmonaco AG, Biamino E, Banaudi E, Carta C, Rossi C, Silengo MC. 2008. Clinical and molecular characterization of 40 patients with Noonan syndrome. Eur J Med Genet 51:566–572.

Hennekam RC. 2003. Costello syndrome: an overview. Am J Med Genet C Semin Med Genet 117:42–48.

Jongmans M, Sistermans EA, Rikken A, Nillesen WM, Tamminga R, Patton M, Maier EM, Tartaglia M, Noordam K, van der Burgt I. 2005. Genotypic and phenotypic characterization of Noonan syndrome: new data and review of the literature. Am J Med Genet A 134A:165–170.

Ko JM, Kim JM, Kim GH, Yoo HW. 2008. PTPN11, SOS1, KRAS, and RAF1 gene analysis, and genotype–phenotype correlation in Korean patients with Noonan syndrome. J Hum Genet 53:999–1006.

Light Y, Paterson H, Marais R. 2002. 14-3-3 antagonizes Ras-mediated Raf-1 recruitment to the plasma membrane to maintain signaling fidelity. Mol Cell Biol 22:4984–4996.

Lo FS, Lin JL, Kuo MT, Chiu PC, Shu SG, Chao MC, Lee YJ, Lin SP. 2008. Noonan syndrome caused by germline KRAS mutation in Taiwan: report of two patients and a review of the literature. Eur J Pediatr 168:919–923.

Mendez HM, Opitz JM. 1985. Noonan syndrome: a review. Am J Med Genet 21:493–506.

Mercer KE, Pritchard CA. 2003. Raf proteins and cancer: B-Raf is identified as a mutational target. Biochim Biophys Acta 1653:25–40.

Musante L, Kehl HG, Majewski F, Meinecke P, Schweiger S, Gillessen-Kaesbach G, Wieczorek D, Hinkel GK, Tinschert S, Hoeltzenbein M, Ropers HH, Kalscheuer VM. 2003. Spectrum of mutations in PTPN11 and genotype–phenotype correlation in 96 patients with Noonan syndrome and five patients with cardio-facio-cutaneous syndrome. Eur J Hum Genet 11:201–206.

Narumi Y, Aoki Y, Niihori T, Sakurai M, Cave H, Verloes A, Nishio K, Ohashi H, Kurosawa K, Okamoto N, Kawame H, Mizuno S, Kondoh T, Addor MC, Coeslier-Dieux A, Vincent-Delorme C, Tabayashi K, Aoki M, Kobayashi T, Guliyeva A, Kure S, Matsubara Y. 2008. Clinical manifestations in patients with SOS1 mutations range from Noonan syndrome to CFC syndrome. J Hum Genet 53:834–841.

Niihori T, Aoki Y, Narumi Y, Neri G, Cave H, Verloes A, Okamoto N, Hennekam RC, Gillessen-Kaesbach G, Wieczorek D, Kavamura MI, Kurosawa K, Ohashi H, Wilson L, Heron D, Bonneau D, Corona G, Kaname T, Naritomi K, Baumann C, Matsumoto N, Kato K, Kure S, Matsubara Y. 2006. Germline KRAS and BRAF mutations in cardio-facio-cutaneous syndrome. Nat Genet 38:294–296.

Noble C, Mercer K, Hussain J, Carragher L, Giblett S, Hayward R, Patterson C, Marais R, Pritchard CA. 2008. CRAF autophosphorylation of serine 621 is required to prevent its proteasome-mediated degradation. Mol Cell 31:862–872.

Pandit B, Sarkozy A, Pennacchio LA, Carta C, Oishi K, Martinelli S, Pogna EA, et al. 2007. Gain-of-function RAF1 mutations cause Noonan and LEOPARD syndromes with hypertrophic cardiomyopathy. Nat Genet 39:1007–1012.

Razzaque MA, Nishizawa T, Komoike Y, Yagi H, Furutani M, Amo R, Kamisago M, Momma K, Katayama H, Nakagawa M, Fujiwara Y, Matsushima M, Mizuno K, Tokuyama M, Hirota H, Muneuchi J, Higashinakagawa T, Matsuoka R. 2007. Germline gain-of-function mutations in RAF1 cause Noonan syndrome. Nat Genet 39:1013–1017.

Reynolds JF, Neri G, Herrmann JP, Blumberg B, Coldwell JG, Miles PV, Opitz JM. 1986. New multiple congenital anomalies/mental retardation syndrome with cardio-facio-cutaneous involvement—the CFC syndrome. Am J Med Genet 25:413–427.

Roberts AE, Araki T, Swanson KD, Montgomery KT, Schiripo TA, Joshi VA, Li L, Yassin Y, Tamburino AM, Neel BG, Kucherlapati RS. 2007. Germline gain-of-function mutations in SOS1 cause Noonan syndrome. Nat Genet 39: 70–74.

Rodriguez-Viciana P, Tetsu O, Tidyman WE, Estep AL, Conger BA, Cruz MS, McCormick F, Rauen KA. 2006. Germline mutations in genes within the MAPK pathway cause cardio-facio-cutaneous syndrome. Science 311:1287–1290.

Schubbert S, Zenker M, Rowe SL, Boll S, Klein C, Bollag G, van der Burgt I, Musante L, Kalscheuer V, Wehner LE, Nguyen H, West B, Zhang KY, Sistermans E, Rauch A, Niemeyer CM, Shannon K, Kratz CP. 2006. Germline KRAS mutations cause Noonan syndrome. Nat Genet 38:331–336.

Tartaglia M, Kalidas K, Shaw A, Song X, Musat DL, van der Burgt I, Brunner HG, Bertola DR, Crosby A, Ion A, Kucherlapati RS, Jeffery S, Patton MA, Gelb BD. 2002. PTPN11 mutations in Noonan syndrome: molecular spectrum, genotype-phenotype correlation, and phenotypic heterogeneity. Am J Hum Genet 70: 1555–1563.

Tartaglia M, Mehler EL, Goldberg R, Zampino G, Brunner HG, Kremer H, van der Burgt I, Crosby AH, Ion A, Jeffery S, Kalidas K, Patton MA, Kucherlapati RS, Gelb BD. 2001. Mutations in PTPN11, encoding the protein tyrosine phosphatase SHP-2, cause Noonan syndrome. Nat Genet 29:465–468.

Tartaglia M, Pennacchio LA, Zhao C, Yadav KK, Fodale V, Sarkozy A, Pandit B, Oishi K, Martinelli S, Schackwitz W, Ustaszewska A, Martin J, Bristow J, Carta C, Lepri F, Neri C, Vasta I, Gibson K, Curry CJ, Siguero JP, Digilio MC, Zampino G, Dallapiccola B, Bar-Sagi D, Gelb BD. 2007. Gain-of-function SOS1 mutations cause a distinctive form of Noonan syndrome. Nat Genet 39:75–79.

van der Burgt I. 2007. Noonan syndrome. Orphanet J Rare Dis 2:4.

Zebisch A, Haller M, Hiden K, Goebel T, Hoefler G, Troppmair J, Sill H. 2009. Loss of RAF kinase inhibitor protein is a somatic event in the pathogenesis of therapy-related acute myeloid leukemias with C-RAF germline mutations. Leukemia 23:1049–1053.

Zebisch A, Staber PB, Delavar A, Bodner C, Hiden K, Fischereder K, Janakiraman M, Linkesch W, Auner HW, Emberger W, Windpassinger C, Schimek MG, Hoefler G, Troppmair J, Sill H. 2006. Two transforming C-RAF germ-line mutations identified in patients with therapy-related acute myeloid leukemia. Cancer Res 66:3401–3408.

Zenker M, Buheitel G, Rauch R, Koenig R, Bosse K, Kress W, Tietze HU, Doerr HG, Hofbeck M, Singer H, Reis A, Rauch A. 2004. Genotype–phenotype correlations in Noonan syndrome. J Pediatr 144:368–374.

Zenker M, Horn D, Wieczorek D, Allanson J, Pauli S, van der Burgt I, Doerr HG, Gaspar H, Hofbeck M, Gillessen-Kaesbach G, Koch A, Meinecke P, Mundlos S, Nowka A, Rauch A, Reif S, von Schnakenburg C, Seidel H, Wehner LE, Zweier C, Bauhuber S, Matejas V, Kratz CP, Thomas C, Kutsche K. 2007a. SOS1 is the second most common Noonan gene but plays no major role in cardio-facio-cutaneous syndrome. J Med Genet 44:651–656.

Zenker M, Lehmann K, Schulz AL, Barth H, Hansmann D, Koenig R, Korinthenberg R, Kreiss-Nachtsheim M, Meinecke P, Morlot S, Mundlos S, Quante AS, Raskin S, Schnabel D, Wehner LE, Kratz CP, Horn D, Kutsche K. 2007b. Expansion of the genotypic and phenotypic spectrum in patients with KRAS germline mutations. J Med Genet 44:131–135.

ELSEVIER

Brain & Development 33 (2011) 166–169

BRAIN & DEVELOPMENT
Official Journal of the Japanese Society of Child Neurology

www.elsevier.com/locate/braindev

Case report

Cardio-facio-cutaneous syndrome with infantile spasms and delayed myelination

Koichi Aizaki [a], Kenji Sugai [a], Yoshiaki Saito [a,*], Eiji Nakagawa [a], Masayuki Sasaki [a], Yoko Aoki [b], Yoichi Matsubara [b]

[a] *Department of Child Neurology, National Center Hospital, National Center of Neurology and Psychiatry (NCNP), 4-1-1 Ogawahigashi-cho, Kodaira, Tokyo 187-8551, Japan*

[b] *Department of Medical Genetics, Tohoku University School of Medicine, 1-1 Seiryo-machi, Sendai 980-8574, Japan*

Received 14 January 2010; received in revised form 25 February 2010; accepted 23 March 2010

Abstract

A girl with cardio-facio-cutaneous (CFC) syndrome due to a *BRAF* gene mutation (c.1454T→C, p.L485S) experienced repetitive epileptic spasms at the corrected age of 4 months. Electroencephalograms revealed hypsarrhythmia, and magnetic resonance imaging identified delayed myelination and a hypoplastic corpus callosum. Various antiepileptic treatments, including adrenocorticotropic hormone therapy, were ineffective, although transient seizure control was achieved by a ketogenic diet and clorazepate dipotassium. However, seizures with epileptic foci at the bilateral posterior temporal areas re-aggravated and remained intractable; severe psychomotor delay persisted. This case indicated that infantile spasms in CFC syndrome can be difficult to control and may be accompanied by severe psychomotor retardation and abnormal myelination.

Keywords: Cardio-facio-cutaneous syndrome; Infantile spasms; *BRAF*; Abnormal myelination

1. Introduction

Cardio-facio-cutaneous (CFC) syndrome is characterized by a distinctive facial appearance, congenital heart defects, ectodermal abnormalities, and psychomotor retardation [1]. *BRAF*, *MEK1*, *MEK2*, and *KRAS*, which are involved in the RAS/mitogen-activated protein kinase (MAPK) pathway, have been identified as the causative genes for CFC syndrome. The RAS-MAPK pathway is essential in regulation of the cell cycle, differentiation, growth, and cell senescence [2]. In particular, *BRAF* mutants are the most common in CFC syndrome; their gene product is highly expressed in the brain and plays important roles in myelination and hippocampus-dependent learning [3,4].

A few recent reports have focused on the neurological symptoms of CFC syndrome, describing the complication of epilepsy and neuroradiological findings in this entity [5,6]. However, detailed information on individual patients, including the treatment course of epilepsy, has not been provided. We here describe a CFC syndrome patient with a *BRAF* gene mutation, who experienced infantile spasms and showed delayed myelination on magnetic resonance imaging (MRI).

2. Case report

A girl was born to nonconsanguineous Japanese parents at 33 weeks of gestation after a pregnancy complicated by polyhydramnios. There was no family history of epilepsy or neuromuscular disease and no previous

* Corresponding author. Tel.: +81 42 341 2711; fax: +81 42 346 1705.

E-mail address: saitoyo@ncnp.go.jp (Y. Saito).

0387-7604/$ - see front matter © 2010 The Japanese Society of Child Neurology. Published by Elsevier B.V. All rights reserved.
doi:10.1016/j.braindev.2010.03.008

pregnancy with spontaneous abortion. Birth weight was 2360 g (+2.1 SD), height 42 cm (−0.1 SD), and head circumference 32 cm (+1.7 SD). The Apgar score was 2 at 1 min and 6 at 5 min, and the patient needed artificial ventilation for several days. Mild laryngomalacia was noted, and cardiac ultrasonography revealed pulmonary valve stenosis, hypertrophic cardiomyopathy, and atrial septal defect. G-band analysis showed a karyotype of 46,XX. Metabolic screening tests of blood amino acids and urine organic acids showed negative results.

The patient was fed by a nasogastric tube because of poor milk intake. Repetitive brief tonic seizures emerged at the corrected age of 2 months and consisted of extension of the trunk, accompanied by staring and a few seconds of ocular bobbing. Asynchronous, high-voltage slow waves with multifocal sharp waves appeared with bilateral parieto-occipital predominance on interictal electroencephalogram (EEG) (Fig. 1A). The epileptic seizures remained intractable despite treatment with valproic acid and vitamin B6. Subsequently, the seizure type changed to tonic spasms in clusters when hypsarrhythmia was noted on EEG. Zonisamide (ZNS), clobazam (CLB), phenobarbital, and adrenocorticotropic hormone (ACTH) therapy (0.01 mg/kg/day for 2 weeks) were also ineffective.

On physical examination at the corrected age of 4 months, her weight was 3950 g (−3.5 SD), height 59 cm (−1.2SD), and head circumference 36 cm (−3.4 SD). She presented with a prominent forehead; a coarse face; a wide, depressed nasal bridge with broad anteverted nares; thick lips; and low-set ears. Her hair was sparse and curly, and cutaneous findings included eczema of the face, skin redundancy in the proximal extremities, and deep palmar and plantar creases. Based on her characteristic facial appearance and cardiac anomalies, CFC syndrome was suspected. The patient manifested with generalized hypotonia and showed scarce responses to auditory or visual stimuli and no purposeful movements of the extremities. Deep tendon reflexes were normal. She did not smile or vocalize during this period and showed continuous laryngeal stridor. Laboratory findings revealed hypogammaglobulinemia but were otherwise unremarkable. MRI of the brain revealed a hypoplastic corpus callosum with moderate brain atrophy, delayed myelination, and an ambiguous corticomedullary boundary in the right posterior temporal lobe (Fig. 2A–C). Magneto-

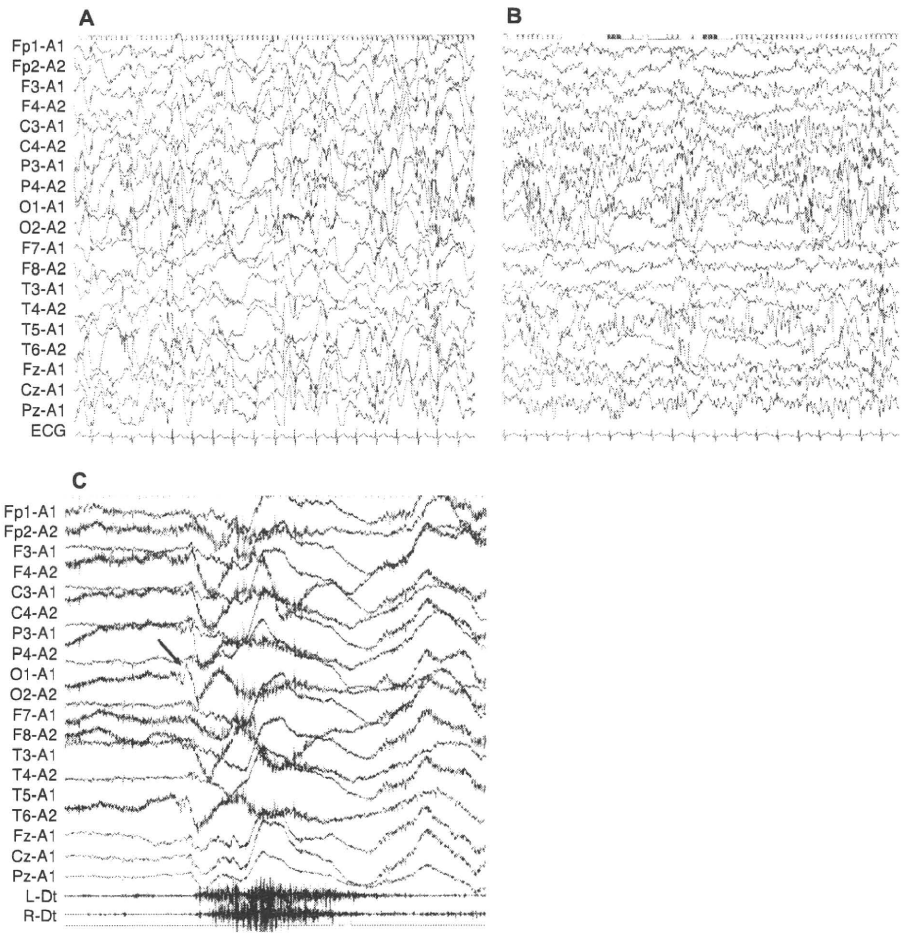

Fig. 1. Electroencephalograms (EEG) of the patient. (A and B) Interictal sleep EEG at the corrected ages of 5 (A) and 9 (B) months. (C) Ictal EEG of epileptic spasms at the corrected age of 5 months. L-Dt, left deltoid muscle; R-Dt, right deltoid muscle.

encephalography identified dipole sources at the bilateral temporo-parietal areas (Fig. 2D). Ictal EEG identified isolated spikes over the right parieto-occipital areas, which heralded the onset of repetitive epileptic spasms (Fig. 1C). Relative hypoperfusion was noted in the left temporo-parietal cortex on interictal single-photon emission computed tomography (SPECT) (Fig. 2E), and subtraction ictal SPECT coregistered to MRI during an episode of brief tonic seizure suggested an epileptic focus in the left temporal cortex (Fig. 2F).

Replacement of ZNS and CLB with potassium bromide (50 mg/kg/day) and topiramate (20 mg/kg/day) and re-administration of ACTH (up to 0.025 mg/kg/day) at the corrected age of 7 months did not improve seizure control. Tonic spasms with oculocephalic deviation in series gradually increased to 10 times per day, and continuous oxygen supply was needed because of recurrent airway infection and increased salivation with frequent desaturation. After initiation of a ketogenic diet with a ketogenic ratio of 3:1 in combination with 0.3 mg/kg/day clorazepate dipotassium, epileptic seizures decreased in frequency by the fifth day and temporarily disappeared at the corrected age of 9 months. Partial improvement in the EEG findings (Fig. 1B) was noted during this period. Her respiratory condition also improved, and thus, oxygen therapy could be terminated. Body weight gradually increased to 6 kg in parallel with improvement in the general condition. However, her development was still stagnated and MRI (Fig. 2A–C) did not show any progress in myelination. Seizures were exacerbated 1 month later and remained intractable.

Based on molecular studies, the patient was finally diagnosed with CFC syndrome. Genetic testing for mutations in *BRAF*, *MEK1*, *MEK2*, *KRAS*, and *HRAS* was performed, and a heterozygous *BRAF* gene mutation (c.1454T→C, p.L485S) was identified.

3. Discussion

Intellectual disabilities in CFC syndrome are more severe than those in Noonan and Costello syndromes, which are also caused by mutations in the constituents of the RAS/MAPK pathway [5,6]. However, the marked developmental delay in the present patient was more serious than that in usual cases of this entity [6]. This may be attributed to the complication of infantile spasms in this patient; the prevalence of this complication in CFC syndrome has been reported to be approximately 10% in large series [5,6]. Clinical information on these previous cases is very limited, and this is the first report on the detailed course of treatment for epileptic encephalopathy. This needs to be recognized to better understand the pathomechanism and management of this syndrome. In the central nervous system, *BRAF* is most densely expressed in hippocampal neurons [4], where the product of this gene is critically involved in the process of long-term potentiation and learning [7]. This preferential distribution may account for the severe psychomotor

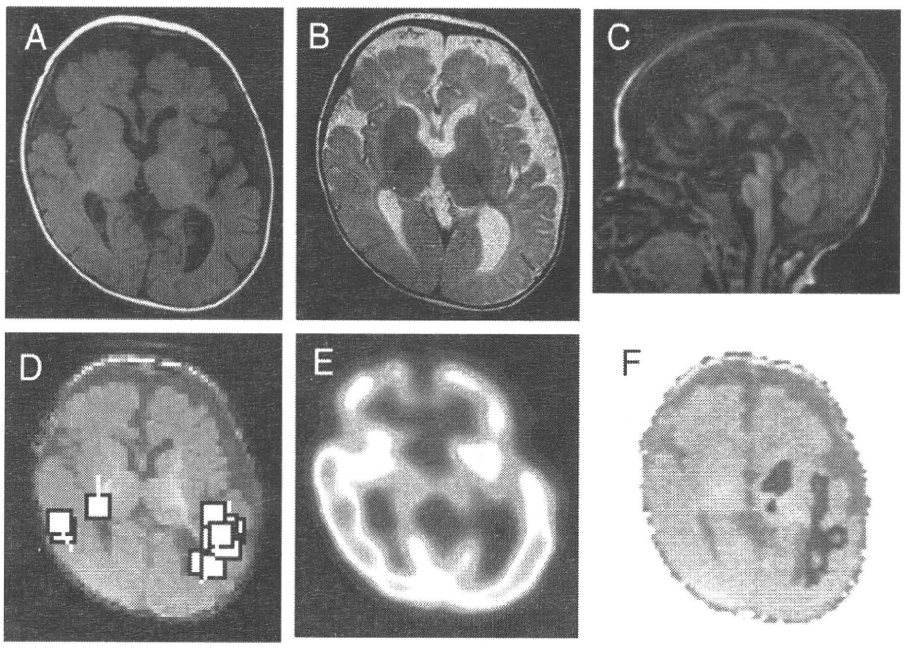

Fig. 2. Neuroimaging of the patient. (A–C) Magnetic resonance images at the corrected age of 9 months. Myelination is visible in the posterior limb of the internal capsule, optic radiation, and deep white matter of the frontal lobe (A and C, T1-weighted images; B, T2-weighted image), which corresponds to the pattern of early infancy. (D–F: examined at the corrected age of 5 months) Magnetic electroencephalogram (D), interictal single-photon emission computed tomography (SPECT) (E), and subtraction of ictal SPECT coregistered to MRI (F) based on a brief tonic seizure.

retardation in CFC syndrome, but the role of this genetic defect in epileptogenesis remains unclear. The presence of brain anomalies, including pachygyria and heterotopia, in CFC syndrome supports the contribution of *BRAF* to the morphogenesis of the brain and may be partly responsible for epilepsy in CFC syndrome. The ambiguous corticomedullary boundary in the right temporal lobe in the present patient may represent cortical dysgenesis in this area, which may have played a role in the evolution of infantile spasms in this patient. We observed another patient with a *BRAF* mutation (c.1495A→G, p.G499E) and lobar dysplasia in the left temporal cortex [8] (initially reported as Noonan syndrome). This suggests a propensity toward involvement of this region in CFC syndrome, possibly through the specific spatial distribution of the *BRAF* gene in corticogenesis and epileptogenesis. Although abundant *BRAF* expression in the fetal cerebrum has been confirmed, further studies on the detailed distribution of this gene in cell populations and cortical regions are required [9].

Another characteristic of the present patient was markedly delayed myelination throughout the course of the disease. Nonspecific delayed myelination and thinning of the corpus callosum are not uncommon findings in infantile spasms, which may be related to the persistence of hypsarrhythmic discharges [10]. However, these findings have also been recognized in some CFC syndrome patients without infantile spasms [5]. Conditional ablation of the *BRAF* gene in neuroglial precursors in mice resulted in severe dysmyelination and defective oligodendrocyte differentiation [3], thus supporting the idea that CFC syndrome can be regarded as a type of myelination disorder. Given that the presence of delayed myelination does not always correlate with seizure control and developmental outcomes in infantile spasms [11], the significance of this MRI finding in epileptogenesis and prognosis of CFC syndrome should be specifically explored.

Another patient with CFC syndrome due to an L485S mutation in the *BRAF* gene, identical to the defect in the present case, also showed infantile spasms [5]. This mutated residue is located in the protein kinase domain, a defect of which would critically affect the activity of BRAF protein. Although some mutations in this domain could result in a less severe phenotype [5], the neurological complications observed in the present patient, i.e., epileptic encephalopathy and abnormal myelination, may be specifically linked to certain genetic defects in CFC syndrome and may be characteristic in patients with a severe phenotype. Further analysis of genotype–phenotype correlations is required in this regard.

References

[1] Niihori T, Aoki Y, Narumi Y, Neri G, Cavé H, Verloes A, et al. Germline KRAS and BRAF mutations in cardio-facio-cutaneous syndrome. Nat Genet 2006;38:294–6.
[2] Aoki Y, Niihori T, Narumi Y, Kure S, Matsubara Y. The RAS/MAPK syndromes: novel roles of the RAS pathway in human genetic disorders. Hum Mutat 2008;29:992–1006.
[3] Galabova-Kovacs G, Catalanotti F, Malzen D, Reyes GX, Zezula J, Herbst R, et al. Essential role of B-raf in oligodendrocyte maturation and myelination during postnatal central nervous system development. J Cell Biol 2008;180:947–55.
[4] Di Benedetto B, Hitz C, Hölter SM, Kühn R, Vogt Weisenhorn DM, Wurst W. Differential mRNA distribution of components of the ERK/MAPK signaling cascade in the adult mouse brain. J Comp Neurol 2007;500:542–56.
[5] Yoon G, Rosenberg J, Blaser S, Rauen KA. Neurological complications of cardio-facio-cutaneous syndrome. Dev Med Child Neurol 2007;49:894–9.
[6] Armour CM, Allanson JE. Further delineation of cardio-facio-cutaneous syndrome: clinical features of 38 individuals with proven mutations. J Med Genet 2008;45:249–54.
[7] Morozov A, Muzzio IA, Bourtchouladze R, Van-Strien N, Lapidus K, Yin D, et al. Rap1 couples cAMP signaling to a distinct pool of p42/44MAPK regulating excitability, synaptic plasticity, learning, and memory. Neuron 2003;39(2):309–25.
[8] Saito Y, Sasaki M, Hanaoka S, Sugai K, Hashimoto T. A case of Noonan syndrome with cortical dysplasia. Pediatr Neurol 1997;17:266–9.
[9] Storm SM, Cleveland JL, Rapp UR. Expression of raf family proto-oncogenes in normal mouse tissues. Oncogene 1990;5:345–51.
[10] Saltik S, Kocer N, Dervent A. Magnetic resonance imaging findings in infantile spasms: etiologic and pathophysiologic aspects. J Child Neurol 2003;18:241–6.
[11] Takano T, Hayashi A, Sokoda T, Sawai C, Sakaue Y, Takeuchi Y. Delayed myelination at the onset of cryptogenic West syndrome. Pediatr Neurol 2007;37:417–20.

CLINICAL REPORT

AMERICAN JOURNAL OF medical genetics

Implications of Prenatal Diagnosis of the Fetus With Both Interstitial Deletion and a Small Marker Ring Originating From Chromosome 5

Hiroyasu Ohashi,[1] Kaoru Suzumori,[1,2]* Yasushi Chisaka,[3] Shinichi Sonta,[1] Tomoko Kobayashi,[4] Yoko Aoki,[4] Yoichi Matsubara,[4] Michiko Sone,[5] and Lisa G. Shaffer[6]

[1]Fetal Life Science Center, Ltd., Nagoya, Japan

[2]Department of Obstetrics and Gynecology, Nagoya City University, Nagoya, Japan

[3]Department of Obstetrics and Gynecology, Tohoku University, Sendai, Japan

[4]Department of Medical Genetics, Tohoku University, Sendai, Japan

[5]Kagawa National Children's Hospital, Zentsuji, Kagawa, Japan

[6]Signature Genomic Laboratories, Spokane, Washington

Received 5 May 2010; Accepted 2 August 2010

We describe a patient with 47,XY,del(5)(p11p13), +mar observed in prenatal screening. We performed analyses including G-banding, multi-color fluorescent in situ hybridization (mFISH) for fetal chromosome detection. After birth array-based comparative genomic hybridization (aCGH), bacterial artificial chromosome (BAC)-FISH was carried out to define the chromosomal changes precisely. The mFISH revealed that a ring chromosome that had originated from chromosome 5. The aCGH showed that this fetus had a terminal duplication, an interstitial deletion, and a pericentromeric duplication of the short arm of chromosome 5. This complex alteration resulted in partial trisomy 5p15.33–p15.31, partial monosomy 5p14.3–p13.2, and partial trisomy 5p12–p11. To clarify these alterations, we performed BAC-FISH using BAC clones related to deleted and duplicated regions, and found that a derivative (der) chromosome 5 showed the presence of hybridization signals from the duplicated region at 5p15.33 and the loss of hybridization signals from the deleted region at 5p14.2. In addition, FISH analysis confirmed the origin of the marker chromosome. Hybridization signals from the second intervening sequence at 5p13.1, between the deleted region and the pericentric duplicated region, were present on the marker ring chromosome. © 2010 Wiley-Liss, Inc.

Key words: BAC-FISH; microarray analysis; prenatal diagnosis; ring chromosome

How to Cite this Article:
Ohashi H, Suzumori K, Chisaka Y, Sonta S, Kobayashi T, Aoki Y, Matsubara Y, Sone M, Shaffer LG. 2011. Implications of prenatal diagnosis of the fetus with both interstitial deletion and a small marker ring originating from chromosome 5.
Am J Med Genet Part A 155:192–196.

INTRODUCTION

When genetic abnormalities are observed during prenatal screening, deletions, and supernumerary ring chromosomes are often seen separately [Gardner and Sutherland, 1996; Ryan et al., 1997; Slavotinek and Kingston, 1997]. Most cases with deletion of autosomes, even that of a tiny segment, are accompanied by clinical symptoms, including mental and developmental retardation; on the other hand, there have been examples of cases with deletion of autosomes without any abnormal features [Gardner and Sutherland, 1996; Daniel and Malafiej, 2003; Liehr et al., 2004].

Here, we describe a rare case with both interstitial deletion and a small ring originating from the same chromosome 5 detected prenatally and characterized by molecular cytogenetics. We emphasize the usefulness of molecular cytogenetics involving array-based comparative genomic hybridization (aCGH) and bacterial artificial chromosome (BAC)-fluorescent in situ hybridization BAC-FISH in providing precise information in cases of complex structural abnormality.

CLINICAL REPORT

Amniocentesis requested for advanced maternal age was performed in gestational week 16 on a 42-year-old woman with two

*Correspondence to:
Kaoru Suzumori, M.D., Ph.D., Fetal Life Science Center, 2-22-8 Chikusa, Chikusa-Ku, Nagoya 464-0858, Japan. E-mail: k.suzumori@flsc.jp
Published online 22 December 2010 in Wiley Online Library (wileyonlinelibrary.com).
DOI 10.1002/ajmg.a.33764

normal children. Fetal chromosomes were analyzed by GTG banding and multi-color fluorescent in situ hybridization (mFISH) using cultured amniocytes. After cytogenetic analyses, she was informed that one chromosome 5 with interstitial deletion and a small marker ring chromosome were detected in all the cells. Then, chromosomal analysis of the parents was performed on peripheral blood and showed normal karyotyes. It was difficult to offer additional molecular analyses within a limited term for pregnancy interruption. Ultrasonographic examination at 19 weeks of gestation did not detect any specific abnormality in the fetus. Despite possible unfavorable prognosis informed in genetic counseling, she and her spouse decided against termination of the pregnancy.

The pregnancy was uneventful and she delivered a phenotypically normal boy at 39 weeks of gestation. Apgar score was 8/8 and there were no particular clinical features. Body length, weight, and head circumference were within the normal range: 48 cm, 2,916 g, and 33 cm, respectively. After birth, we received informed consent to examine aCGH and BAC-FISH for further confirmation of the diagnosis.

Developmental, physical, and neurological examinations were normal and he appropriately reached his milestones. At 1 year and 6 months, his developmental quotient (DQ) was 110 (Fig. 1); echocardiography and brain imaging were also normal.

MOLECULAR CYTOGENETICSTUDIES

Chromosome and FISH Analyses

Cultured amniocytes were analyzed using G-banding with 540 bands per haploid number. G-banded chromosomes demonstrated

FIG. 1. Propositus at age 8 months (left picture) and 1 year 6 months (right picture). Note the phenotypically normal boy.

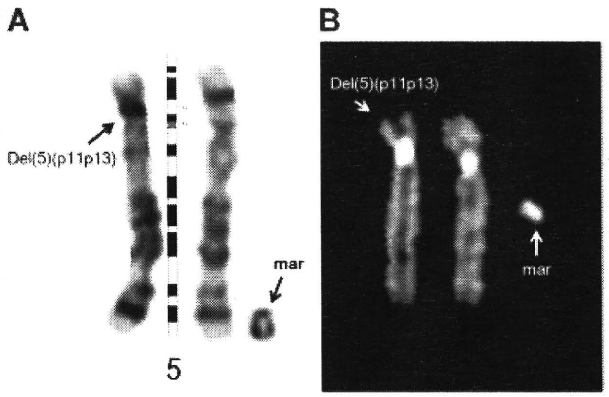

FIG. 2. Partial karyogram of chromosome 5, del(5p), and supernumerary ring by G-banding (A) and mFISH (B).

that all cells had an interstitial deletion of chromosome 5 (5p11 → p13), and a small marker ring chromosome (Fig. 2A). The origin of this marker chromosome was unclear by G-banding. Therefore, the initial karyotyping was 47,XY,del(5)(p11p13), +mar. The mFISH revealed that the marker ring originated from chromosome 5, the same as the deleted chromosome (Fig. 2B). The ring chromosome seemed to have a centromere because this marker was detected in all cells. Chromosome analysis of the parents showed no abnormalities, indicating that these structural abnormalities in the fetus were de novo.

Oligonucelotide aCGH

For detection of gain and loss of chromosome segments, oligonucleotide-based microarray analysis was performed on reserved cultured amniocytes using a 105K-feature whole-genome microarray (Signature Chip Oligo Solution®, made for Signature Genomic Laboratories by Aligent Technologies Inc., Santa Clara, CA) [Ballif et al., 2008]. Microarray analysis of 1543 loci using on oligonucleotide array detected a complex abnormality in the DNA obtained from cultured amniocytes. Based on microarray analysis, this fetus had two duplications and a deletion of the short arm of chromosome 5. This abnormality was first characterized by a single copy gain of 380 oligonucleotide probes from the terminal end of the short arm of 5p, at 5p15.33p15.31. The extent of this duplication has been estimated to be approximately 6.1 Mb. The second alteration was characterized by a single copy loss of 347 oligonucleotide probes from 5p14.3p13.2. The extent of this interstitial deletion is estimated to be approximately 15.3 Mb. The third alteration was characterized by a single copy gain of 147 oligonucleotide probes from the pericentric region at 5p12p11. The extent of this duplication has been estimated to be approximately 3.4 Mb. Thus, this complex alteration resulted in partial trisomy 5p15.33–p15.31, partial monosomy 5p14.3–p13.2, and partial trisomy 5p12–p11. In conclusion, the result of microarray was arr5p15.33–p15.31(131,945–6,267,160)x3, 5p14.3–p13.2(21,438,495–36,736,934)x1, 5p12–p11(42,529,343–45,908,725)x3 (Fig. 3).

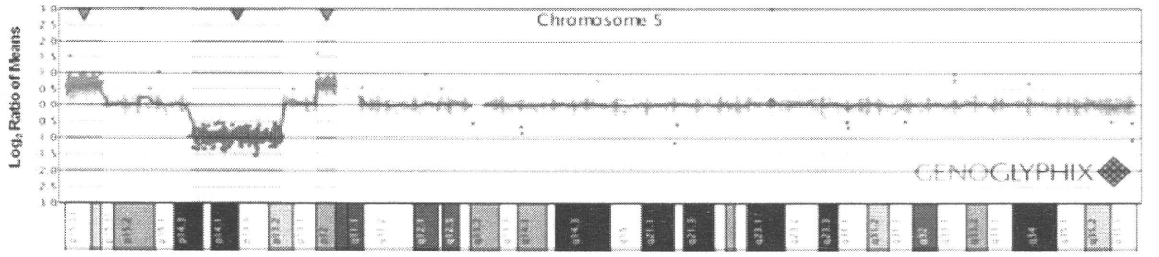

FIG. 3. Microarray plot showing, from left to right, a single copy gain of 380 oligonucleotide probes at 5p15.33p15.31, approximately 6.1 Mb in size; a single copy loss of 347 oligonucleotide probes from 5p14.3p13.2, approximately 15.3 Mb; and single copy gain of 147 oligonucleotide probes at 5p12p11, approximately 3.4 Mb in size. Probes are ordered on the x-axis according to physical mapping positions, with the distal p-arm on the left and the distal q-arm on the right.

BAC-FISH

For confirmation of the array results, FISH analyses were performed with BAC clones from duplicated and deleted regions as previously described [Shaffer et al., 1994; Traylor et al., 2009]. For this study, we used cord blood obtained at delivery.

FISH using a BAC clone from the 5p14.2 deleted region (RP11-701M20) and the 5p15.33 duplicated region (RP11-1006P13) identified an abnormal deleted (del) chromosome 5 that showed the loss of hybridization signals from the deleted region at 5p14.2 (Fig. 4A) and the presence of hybridization signals from the duplicated region at 5p15.33 (Fig. 4C). Interphase FISH

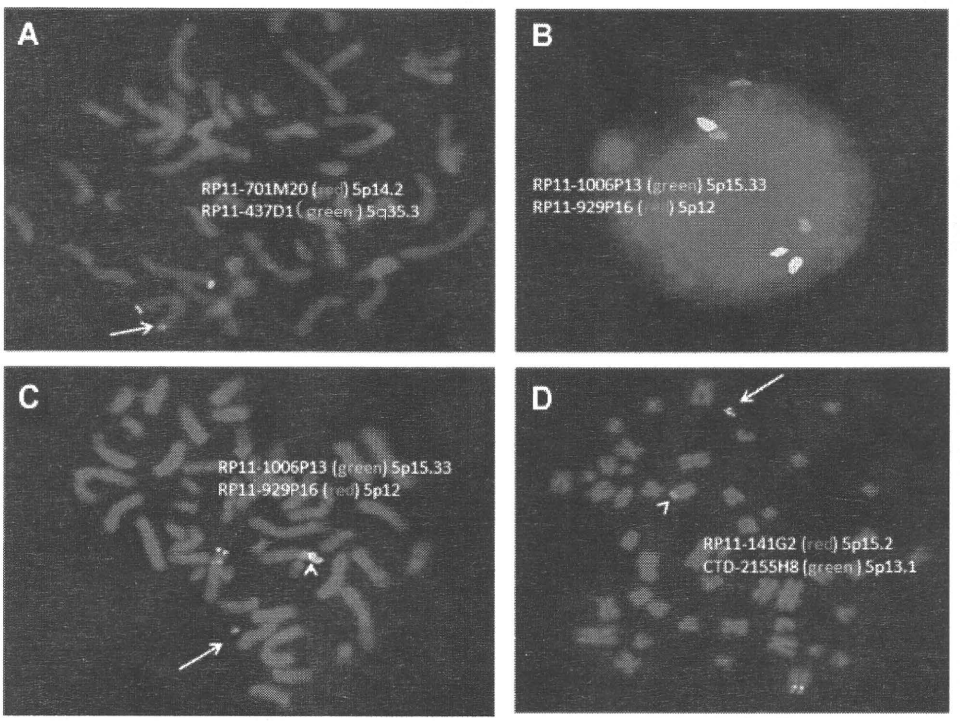

FIG. 4. FISH characterizations of a complex rearrangement on the short arm of chromosome 5. A: FISH showing a deletion of 5p14.2, BAC clone RP11-701M20 from 5p14.2 is labeled in red, and RP11-437D1 from 5q35.3 is labeled in green as a control. The presence of one red signal indicates deletion of 5p14.2 on one homologue (arrow). B,C: FISH with probes from the two regions is shown to be present in three copies by aCGH. BAC clone RP11-1006P13 from 5p15.33 is labeled in green, and RP11-929P16 from 5p12 is labeled in red. Interphase FISH (B) confirmed the presence of three copies of both regions. Metaphase FISH (C) shows a red signal but not a green signal on a small, supernumerary ring chromosome (arrow), indicating the presence of the 5p12 material on the supernumerary chromosome. Dotted green signals from 5p15.33 were present on the normal chromosome 5 homologs, but terminal duplicated signals were observed on one chromosome 5 (arrow head). D: FISH with probes from the intervening regions shown to be present in two copies by aCGH. BAC clone RP11-141G2 from 5p15.2 is labeled in red, and CTD-2155H8 from 5p13.1 is labeled in green. The supernumerary ring chromosome (arrow) shows a green signal and therefore the presence of material from 5p13.1, while one chromosome 5 homolog (arrowhead) shows a deletion for this region. The probe from 5p15.2 shows a normal hybridization pattern.

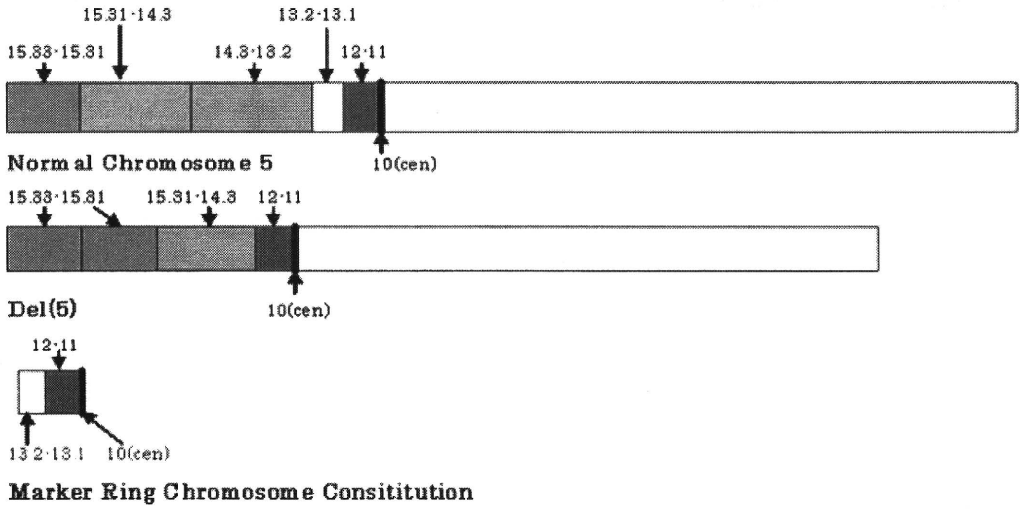

FIG. 5. Molecular background information on the deleted chromosome 5 and marker ring chromosome.

(Fig. 4B) clarified the presence of three copies of 5p15.33 and 5p12 regions. This del(5) also showed hybridization signals in an experiment using BAC clones from the first normal intervening sequence, between the terminal duplication and the deleted region, at 5p15.2 (RP11-141G2; Fig. 4D). Additional FISH analysis using a BAC clone from the 5p12 duplicated region (RP11-929P16) confirmed the origin of the marker ring chromosome (Fig. 4C). Hybridization signals from the second intervening normal sequence at 5p13.1 (CTD-2155H8), between the deleted region and the pericentric duplicated region, were also present on the marker ring chromosome, but not on the del(5), indicating that the deletion on that chromosome extends from 5p14.3 through 5p13.1 (Fig. 4D).

In conclusion, this baby had two abnormal derivative chromosomes. The first der(5) had an abnormal short arm with a duplication of 5p15.31 → 5p15.33, and a deletion of 5p13.1 → p14.3. The second der(5), the marker ring chromosome, was comprised of material from 5p10 → p13.2 (Fig. 5). The final karyotype of the baby is: 47,XY,ish der(5)(pter → p15.31::pter → p14.3::p11 → qter)(RP11-1006P13++,RP11-141G2+,RP11-701M20−,CTD-2155H8−),+der(5)(:13.2 → p10:)(CTD-2155H8+,RP11-929P16+).

DISCUSSION

Partial deletion of 5p is often seen in prenatal diagnoses and newborn analyses [Mainardi et al., 2001; Weiss et al., 2003]. In autosomes other than chromosome 5, deletions involving various chromosomes have also been reported in the literature [Gardner and Sutherland, 1996; Ryan et al., 1997; Slavotinek and Kingston, 1997]. Partial deletion of autosomes is generally accompanied by mild-to-severe clinical symptoms, including mental and developmental retardation in babies, although there have been exceptional cases where no clinical symptoms are observed [Callen et al., 1993; Overhauser et al., 1994; Knight et al., 1995]. Supernumerary marker chromosomes including small rings are also seen frequently in prenatal diagnoses [Michalski et al., 1993; Brøndum-Nielsen and Mikkelsen, 1995; Karaman et al., 2006]. Among babies with such small markers, some cases have no clinical features, but others showed mild-to-severe abnormalities after birth [Callen et al., 1993; Overhauser et al., 1994; Knight et al., 1995; Gardner and Sutherland, 1996; Daniel and Malafiej, 2003; Liehr et al., 2004; Bernardini et al., 2007]. Thus, in genetic counseling, it is important to offer chromosomal information from prenatal diagnoses and to provide as much detail as possible, including the origin and inheritance.

The present case had a deletion and a supernumerary marker ring chromosome. To our knowledge, this is the first report of detection by prenatal screening of both a deletion and a marker ring. In the literature, there are some mosaic cases of clones with a deletion and an additional ring separately [Gutiérrez-Angulo et al., 2002; Gereltzul et al., 2008; Kara et al., 2008], but such cases are extremely rare. In newborn infants, only one other case has been reported [Schuffenhauer et al., 1996] with a deletion and a ring of chromosome 5; this baby showed a mosaicism of 46,XY,del(5)/47,XY, del(5),+dic(5), with macrocephaly, asymmetric square skull, minor facial anomalies, omphalocele, inguinal hernias, hypospadias, and club feet. The break points of the deletion shared cen and p13 with those of the dicentric ring chromosome; this case had partial duplication of 5p (p13 → cen), and the mechanisms of del(5) and dic(5) were relatively straightforward. In the present case, on the other hand, the mechanisms of del(5) and marker ring [r(5)] were extremely complex. Microarray analysis revealed a terminal duplication, an interstitial deletion, and a pericentromeric duplication of the short arm of chromosome 5. Through this analysis, a total of six break points of the short arm of chromosome 5 (p15.33, p15.31, p14.3, p13.2, p12, and p11) were related to the formation of the structural abnormality with the duplication and the deletion, and the marker ring. According to the results of the G-band analysis of this case, we determined the break points of del(5) to be p11 and p13. However, assuming the microarray data are correct, the composition of r(5) becomes complicated, and explanation of the underlying mechanisms becomes difficult. To facilitate understanding of the exact composition of del(5) and r(5),

we performed FISH analysis using BAC clones from the duplicated 5p15.33, 5p12 regions and deleted 5p14.2 region. The short arm of the del(5) revealed a duplication of 5p15.31 → 5p15.33 and a deletion of 5p13.1 → p14.3. The r(5) was comprised of material from 5p10 → p13.2. Although supernumerary ring chromosome formation is difficult to determine, we speculate that this case have resulted from "centromere misdivision" along with a break in either the p or q arm, forming a small ring chromosome [Baldwin et al., 2008].

In summary, this complex 5p abnormality was characterized by a terminal duplication of 5p15.33p15.31 of approximately 6.4 Mb, an interstitial deletion 15p14.3p13.2 of approximately 15.3 Mb and an interstitial duplication of 5p12p11 of approximately 3.4 Mb. The 5p terminal duplication contained at least 21 genes including ADAMTS16, AHRR, and C5orf38. The 5p14.3p13.2 deletion lacked at least 22 genes including *CDH12*, *PRDM9*, *CDH10*, and *DH9*. The 5p12p11 duplication contained at least 11 genes including *GHR*, *SEPP1*, *C5orf39*, and *ZNF11131*.

When the child was examined at 1 year and 6 months, we could not find any developmental abnormality, either physical or mental. Because of his age he will need to be followed to confirm normal intellectual development. In order to provide accurate and useful genetic counseling in similar cases in the future, the accumulation of further reports with complicated chromosome abnormalities would be beneficial.

REFERENCES

Baldwin EL, May LE, Justice AN, Martin CL, Ledbetter DH. 2008. Mechanism and consequences of small supernumerary marker chromosomes: From Barbara McClintock to modern genetic-counseling issue. Am J Hum Genet 82:398–410.

Ballif BC, Theisen A, McDonald-McGinn DM, Zackai EH, Bejjanni BA, Shaffer LG. 2008. Identification of a previously unrecognized microdeletion syndrome of 16q11.2q12.2. Clin Genet 74:469–475.

Bernardini L, Capalbo A, D'Avanzo MG, Torrente I, Grammatico P, Dell'Edera D, Cavalcanti DP, Novelli A, Dallapiccola B. 2007. Five cases of supernumerary small ring chromosomes 1: Heterogeneity and genotype–phenotype correlation. Eur J Med Genet 50:94–102.

Brøndum-Nielsen K, Mikkelsen M. 1995. A 10-year survey, 1980–1990, of prenatally diagnosed small supernumerary marker chromosomes, identified by FISH analysis. Outcome and follow-up of 14 cases diagnosed in a series of 12,699 prenatal samples. Prenat Diagn 15:615–619.

Callen DF, Eyre H, Lane S, Shen Y, Hansmann I, Spinner N, Zackai E, McDonald-McGinn D, Schuffenhauer S, Wauters J, Van Thienen M-N, Van Roy B, Sutherland GR, Haan EA. 1993. High resolution mapping of interstitial long arm deletions of chromosome 16: Relationship to phenotype. J Med Genet 30:828–832.

Daniel A, Malafiej P. 2003. A series of supernumerary small ring marker autosomes identified by FISH with chromosome probe arrays and literature review excluding chromosome 15. Am J Med Genet Part A 117A:212–222.

Gardner RJM, Sutherland GR. 1996. Chromosome Abnormalities and Genetic Counseling. 2nd edition. New York, Oxford: Oxford University Press. pp. 1–478.

Gereltzul E, Baba Y, Suda N, Shiga M, Inoue MS, Tsuji M, Shin I, Hirata Y, Ohyama K, Moriyama K. 2008. Case report of de novo dup(18p)/del-(18q) and r(18) mosaicism. J Hum Genet 53:941–946.

Gutiérrez-Angulo M, Lazalde B, Vasquez AI, Leal C, Corral E, Rivera H. 2002. del(X)(p22.1)/r(X)(p22.1q28) Dynamic mosaicism in a Turner syndrome patient. Ann Genet 45:17–20.

Kara N, Okten G, Gune SO, Saglam Y, Tasdemir HA, Pinarli FA. 2008. An epileptic case with mosaic ring chromosome 6 and 6q terminal deletion. Epilepsy Res 80:219–223.

Karaman B, Aytan M, Yilmaz K, Toksoy G, Onal EP, Ghanbari A, Engur A, Kayserili H, Yuksel-Apak M, Basaran S. 2006. The identification of small supernumerary marker chromosomes; the experiences of 15,792 fetal karyotyping from Turkey. Eur J Med Genet 49:207–214.

Knight LA, Yong MH, Tan M, Ng IS. 1995. Del(3) (p25.3) without phenotypic effect. J Med Genet 32:994–995.

Liehr T, Claussen U, Starke H. 2004. Small supernumerary marker chromosomes (sSMC) in humans. Cytogenet Genome Res 107:55–67.

Mainardi PC, Perfumo C, Calì A, Coucourde G, Pastore G, Cavani S, Zara F, Overhauser J, Pierluigi M, Bricarelli FD. 2001. Clinical and molecular characterization of 80 patients with 5p deletion: Genotype–phenotype correlation. J Med Genet 38:151–158.

Michalski K, Rauer M, Williamson N, Perszyk A, Hoo JJ. 1993. Identification, counselling, and outcome of two cases of prenatally diagnosed supernumerary small ring chromosomes. Am J Med Genet 46:88–94.

Overhauser J, Huang X, Gersh M, Wilson W, McMahon J, Bengtsson U, Rojas K, Meyer M, Wasmuth JJ. 1994. Molecular and phenotypic mapping of the short arm of chromosome 5: Sublocalization of the critical region for the cri-du-chat syndrome. Hum Mol Genet 3:247–252.

Ryan AK, Goodship JA, Wilson DI, Philip N, Levy A, Seidel H, Schuffenhauer S, Oechsler H, Belohradsky B, Prieur M, Aurias A, Raymond FL, Clayton-Smith J, Hatchwell E, McKeown C, Beemer FA, Dallapiccola B, Novelli G, Hurst JA, Ignatius J, Green AJ, Winter RM, Brueton L, Brøndum-Nielsen K, Stewart F, Van Essen T, Patton M, Paterson J, Scambler PJ. 1997. Spectrum of clinical features associated with interstitial chromosome 22q11 deletions: A European collaborative study. J Med Genet 34:798–804.

Schuffenhauer S, Kobelt A, Daumer-Haas C, Löffler C, Müller G, Murken J, Meitinger T. 1996. Interstitial deletion 5p accompanied by dicentric ring formation of the deleted segment resulting in trisomy 5p13-cen. Am J Med Genet 65:56–59.

Shaffer LG, McCaskill C, Han J-Y, Choo KHA, Cutillo DM, Donnenfeld AE, Weiss L, Van Dyke DL. 1994. Molecular characterization of de novo secondary trisomy 13. Am J Hum Genet 55:968–974.

Slavotinek A, Kingston H. 1997. Interstitial deletion of bands 4q12 → q13.1: Case report and review of proximal 4q deletions. J Med Genet 34:862–865.

Traylor R, Fan Z, Ballif BC. 2009. Micordeletion of 6q16.1 encompassing EPHA7 in a child with mild neurological abnormalities and dysmorphic features: Case report. Mol Cytogenet 2:1–6.

Weiss A, Shalev S, Weiner E, Shneor Y, Shalev E. 2003. Prenatal diagnosis of 5p deletion syndrome following abnormally low maternal serum human chorionic gonadotrophin. Prenat Diagn 23:572–574.

Journal of Human Genetics (2011) 56, 34–40

www.nature.com/jhg

ORIGINAL ARTICLE

A genome-wide association study identifies *RNF213* as the first Moyamoya disease gene

Fumiaki Kamada[1], Yoko Aoki[1], Ayumi Narisawa[1,2], Yu Abe[1], Shoko Komatsuzaki[1], Atsuo Kikuchi[3], Junko Kanno[1], Tetsuya Niihori[1], Masao Ono[4], Naoto Ishii[5], Yuji Owada[6], Miki Fujimura[2], Yoichi Mashimo[7], Yoichi Suzuki[7], Akira Hata[7], Shigeru Tsuchiya[3], Teiji Tominaga[2], Yoichi Matsubara[1] and Shigeo Kure[1,3]

Moyamoya disease (MMD) shows progressive cerebral angiopathy characterized by bilateral internal carotid artery stenosis and abnormal collateral vessels. Although ~15% of MMD cases are familial, the MMD gene(s) remain unknown. A genome-wide association study of 785 720 single-nucleotide polymorphisms (SNPs) was performed, comparing 72 Japanese MMD patients with 45 Japanese controls and resulting in a strong association of chromosome 17q25-ter with MMD risk. This result was further confirmed by a locus-specific association study using 335 SNPs in the 17q25-ter region. A single haplotype consisting of seven SNPs at the *RNF213* locus was tightly associated with MMD ($P=5.3\times10^{-10}$). *RNF213* encodes a really interesting new gene finger protein with an AAA ATPase domain and is abundantly expressed in spleen and leukocytes. An RNA *in situ* hybridization analysis of mouse tissues indicated that mature lymphocytes express higher levels of *Rnf213* mRNA than their immature counterparts. Mutational analysis of *RNF213* revealed a founder mutation, p.R4859K, in 95% of MMD families, 73% of non-familial MMD cases and 1.4% of controls; this mutation greatly increases the risk of MMD ($P=1.2\times10^{-43}$, odds ratio=190.8, 95% confidence interval=71.7–507.9). Three additional missense mutations were identified in the p.R4859K-negative patients. These results indicate that *RNF213* is the first identified susceptibility gene for MMD.
Journal of Human Genetics (2011) **56**, 34–40; doi:10.1038/jhg.2010.132; published online 4 November 2010

INTRODUCTION

'Moyamoya' is a Japanese expression for something hazy, such as a puff of cigarette smoke drifting in the air. In individuals with Moyamoya disease (MMD), there is a progressive stenosis of the internal carotid arteries; a fine network of collateral vessels, which resembles a puff of smoke on a cerebral angiogram, develops at the base of the brain (Figure 1a).[1,2] This steno-occlusive change can cause transient ischemic attacks and/or cerebral infarction, and rupture of the collateral vessels can cause intracranial hemorrhage. Children under 10 years of age account for nearly 50% of all MMD cases.[3]

The etiology of MMD remains unclear, although epidemiological studies suggest that bacterial or viral infection may be implicated in the development of the disease.[4] Growing attention has been paid to the upregulation of arteriogenesis and angiogenesis associated with MMD because chronic ischemia in other disease conditions is not always associated with a massive development of collateral vessels.[5,6] Several angiogenic growth factors are thought to have functions in the development of MMD.[7]

Several lines of evidence support the importance of genetic factors in susceptibility to MMD.[8] First, 10–15% of individuals with MMD have a family history of the disease.[9] Second, the concordance rate of MMD in monozygotic twins is as high as 80%.[10] Third, the prevalence of MMD is 10 times higher in East Asia, especially in Japan (6 per 100 000 population), than in Western countries.[3] Familial MMD may be inherited in an autosomal dominant fashion with low penetrance or in a polygenic manner.[11] Linkage studies of MMD families have revealed five candidate loci for an MMD gene: chromosomes 3p24–26,[12] 6q25,[13] 8q13–24,[10] 12p12–13[10] and 17q25.[14] However, no susceptibility gene for MMD has been identified to date.

We collected 20 familial cases of MMD to investigate linkage in the five putative MMD loci. However, a definitive result was not obtained for any of the loci. We then hypothesized that there might be a founder mutation among Japanese patients with MMD because the prevalence of MMD is unusually high in Japan.[15] Genome-wide and locus-specific association studies were performed and successfully identified a single gene, *RNF213*, linked to MMD. We report here a strong association between MMD onset and a founder mutation in *RNF213*, as well as the expression profiles of *RNF213*, in various tissues.

[1]Department of Medical Genetics, Tohoku University School of Medicine, Sendai, Japan; [2]Department of Neurosurgery, Tohoku University School of Medicine, Sendai, Japan; [3]Department of Pediatrics, Tohoku University School of Medicine, Sendai, Japan; [4]Department of Pathology, Tohoku University School of Medicine, Sendai, Japan; [5]Department of Microbiology and Immunology, Tohoku University School of Medicine, Sendai, Japan; [6]Department of Organ Anatomy, Yamaguchi University Graduate School of Medicine, Ube, Japan and [7]Department of Public Health, Graduate School of Medicine, Chiba University, Chiba, Japan
Correspondence: Dr S Kure, Department of Pediatrics, Tohoku University School of Medicine, 1-1 Seiryo-machi, Aoba-ku, Miyagi, Sendai 980-8574, Japan.
E-mail; kure@med.tohoku.ac.jp
Received 30 September 2010; accepted 1 October 2010; published online 4 November 2010